Spring 2016

Colloidal Self-Assembly of Multi-fluorescent Silsesquioxane Microparticles

Niharika Neerudu Sreeramulu
Western Kentucky University, niharika.neerudu452@topper.wku.edu

COLLOIDAL SELF-ASSEMBLY OF MULTI-FLUORESCENT SILSESQUIOXANE MICROPARTICLES

A Thesis
Presented to
The Faculty of the Department of Chemistry
Western Kentucky University
Bowling Green, Kentucky

In Partial Fulfillment
Of the Requirements for the Degree
Master of Science

By
Niharika Neerudu Sreeramulu

May 2016

COLLOIDAL SELF-ASSEMBLY OF MULTI-FLUORESCENT SILSESQUIOXANE MICROPARTICLES

Date Recommended 04/21/2016

H. P. Rathnayake

Dr. Hemali Rathnayake, Director of Thesis

Dr. Edwin Stevens

Dr. Moon-Soo Kim

Dean, Graduate School

4/26/16

Date

ACKNOWLEDGEMENT

I would like to express my sincere gratitude and appreciation to my research advisor Dr. Hemali Rathnayake for all her support and guidance towards my research. Without her it would be impossible for me to come this far. I appreciate her patience and effort in teaching me from the C of Chemistry. She is one of the geniuses in synthesizing nanoparticles and I have learned a lot from her. She inspires and motivates me to look forward more in chemistry. I appreciate for all her dedication towards me during my research. I wouldn't have come this far without her.

I would also like to thank Dr. John Andersland for his enormous support and help in training me on the most valuable technique of electron microscopy and for all his guidance towards the future. I would like to thank Pauline Norris for her help and support for the elemental analysis at the Advance Material Institute and Dr. Houyin Zhao for her help in XRD and TGA at the Thermal Analysis Lab. Without these people my thesis data would have been incomplete. Also my research was greatly helped by John T. Ferguson. I would like to express my sincere gratitude to Dr. Edwin Stevens for serving me as my thesis reader and also helping me in understanding and interpreting the XRD data and Dr. Moon-Soo Kim for serving me on my committee. Also I would like to thank everyone in my research group for their help and support directly or indirectly.

Finally I would like to thank my family and friends for their endless support and encouragement. My parents are my backbone for all my achievements.

CONTENTS

LIST OF FIGURES

Figure **Page**

LIST OF SCHEMES

LIST OF TABLES

Table **Page**

COLLOIDAL SELF-ASSEMBLY OF MULTI-FLUORESCENT SILSESQUIOXANE MICROPARTICLES

Niharika Neerudu Sreeramulu May 2016 81 pages

Directed By: Dr. Hemali Rathnayake, Edwin Stevens, and Moon-Soo Kim

Department of Chemistry Western Kentucky University

Self-assembly of colloidal microparticles is one of the strategies for making characteristic patterns. These versatile self-assemblies provide a route to elevate the efficiency of an electronic device. Silsesquioxane particles with various functionalities were synthesized by a modified Stöber condensation method. This thesis describes the synthesis of benzylchloride silsesquioxanes, benzylchloride-amine silsesquioxanes and amine-functionalized silsesquioxane particles with multi-fluorescent tags. The size and morphology of the particles were controlled by varying the concentration of base and anhydrous ethanol (solvent). The size distribution of particles was controlled by adjusting the molar ratios of organotrialkoxy silane, base, and ethanol concentrations. Through selective post-functionalization with fused arenes of anthracene and rhodamine, multi-fluorescent particles were obtained. Morphologies and optical properties of particles were characterized by TEM, SEM, fluorescence optical microscopy, and absorption and fluorescence spectroscopies. The composition of silsesquioxanes was confirmed by FTIR, thermogravimetric analysis, and elemental analysis. A versatile technique was developed for the self-assembly of particles on different polymer substrates by changing the colloidal suspension concentration and the polymer substrate.

CHAPTER 1

INTRODUCTON

1.1 Overview

Organic-inorganic hybrid nanoparticles/nanostructures of the silsesquioxane family are receiving much interest due to their enormous range of applications from electronics to biomedical materials due to their rigid and thermally stable silsesquioxane core. Silsesquioxanes belong to a family of polyoligomeric silsesquioxanes. Silsesquioxanes are generally a cage like structures, where mostly the structures are in the shapes of cube, hexagonal prism, octagonal prism, or open caged like structures. Synthesis of these organic-inorganic hybrid nanoparticles with controlled size ranging from nanometer scale to micrometer scale is a challenge using current sol-gel synthesis methods. Researchers have reported that the cubic or cage silsesquioxanes are more preferable, but due to their complicated synthetic procedures and divergent size ranges, new methods need to be developed for the synthesis of silsesquioxane nanoparticles/nanostructures to produce more uniform size and properties distributions.[1]

The sol-gel method is the most widely used synthetic method, which involves hydrolysis and condensation of the alkoxide precursor in an aqueous medium.[2] The sol-gel method also involves acid or base catalysed hydrolysis and condensation reactions which forms silica polymers[3] with Si-O-Si networks, significant linkages of a silsesquioxanes. The above method has limitations on ligand incorporation, and many recent developments have occurred in the synthesis of silsesquioxanes. Recently developed methods include the hydrolytic condensation reaction, co-

condensation of tetraethoxysilane with organotrialkoxysilanes[4], and grafting techniques using Stöber silica particles.[2] Most of these methods face problems in controlling the particle size and morphology or low ligand incorporation to the core.

Previously researchers have used the modified Stöber method to prepare organically modified silsesquioxanes of submicron size using tetraethoxysilane and organotrialkoxy silane precursors.[2] The disadvantages of the above synthesis was low ligand incorporation due to the fact that the core structure was still silica. Periphery and core functionalization is possible, but there is still less ligand incorporation. We propose a method to synthesize silsesquioxanes where high ligand incorporation is possible due to use of silsesquioxane core with organic groups. Both periphery and core functionalization is possible and also any organic ligands can be introduced via synthetic modifications.

Self-assembly of colloidal microparticles is one strategy for making desired characteristic patterns.[5] Colloidal self-assembled crystals have wide applications in electronic devices, as a template for fabrication, as photonic crystals, etc. Recently many methods have been developed to prepare a variety of colloidal self-assembly crystals for various applications, depending on the functionality of the colloids and the substrates used. All the techniques used to date have their own advantages and disadvantages, but the spin coating technique is one of the most widely used.

The spin coating method for the self-assembly of colloids has gained importance because it is a fast and reproducible method. The self-assembly of colloids achieved via spin coating is promising, and has wide application in coatings, adhesives, preparing thin films in electronics, etc.[7.] The shape and sizes of these colloidal

crystals formed via spin coating depend on the spin speed, interactions of the colloids with the substrates, concentration of the colloidal suspension and also the functionality of the colloids. Control these factors during self-assembly is a challenge for researchers.

1.2 General goal of research

The focus of my research work has been to synthesize multi-functionalized silsesquioxane particles using different silane precursors and self-assemble particles via dipole-dipole interactions on different polymer substrates via the spin coating technique. This thesis describes the synthesis of three different types of silsesquioxane particles which are functionalized with reactive organic groups and post functionalized with fluorescent dyes.

The second goal of the research has been to develop a technique for the self-assembly of silsesquioxane particles on different polymer substrates and to study the thin film morphologies of the assemblies. Two different polymers have been used to check the interactions of the particles with the polymer substrate. By mimicking the polymer-particle interactions, our goal is to create ordered microstructures (patterns) on polymer substrate for future use in electronic devices.

CHAPTER 2

BACKGROUND

2.1 Theoretical basis of silsesquioxanes

Silsesquioxanes (SSQ's) are organosilicon compounds with the empirical formula $(RSiO_{1.5})_n$, where R stands for substituent groups such as methyl, ethyl, vinyl, propyl, allyl, phenyl, aminopropyl, etc. The term silsesquioxanes is derived from the terms 'sil' meaning silicon, 'sesqui' means one and a half, and 'oxane' meaning oxygen, when combined together indicates the ratio of silicon: oxygen atoms of 1:1.5.[8] There are unlimited types of SSQ's based on the type of R group used, such as olefins, amines, imides, epoxes, thiols silanols, siloxides, etc.[15] A large number of SSQ's have been developed with different functional groups, numbers of substituent groups, and cage structures.[1]

Accordingly, different structures of SSQ's include polyhedral structures, ladder-type structures (Figure 2.1), open structures, linear structures, and various combinations of these structures.[1] Due to their highly stable silica core and flexibility of modifying the organic groups into the core, SSQ's have proven useful in a wide range of applications from electronics to biomedical materials.

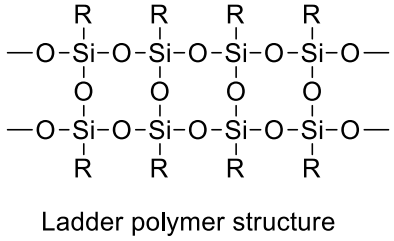

Figure 2.1: Ladder type silsesquioxane structure

2.1.1 Principles involved in preparation of silsesquioxanes

Silsesquioxanes are commonly synthesized by the sol-gel method, which involves hydrolysis and condensation of the organoalkoxy precursors in an aqueous medium.[2] The sol-gel method also involves acid or base catalyzed hydrolysis and condensation reactions which forms silica polymers[3] with Si-O-Si networks, which are significant linkages of silsesquioxanes. Recently most researchers have found the sol-gel process to be limited usefulness. However, there have been advancements in the synthesis of silsesquioxanes in recent years by researchers that used pre-synthesized Stöber silica particles and a grafting technique to graft the desirable organic groups onto the surface of silica particles to prepare organically modified silica.[9,10] However, the grafting of these silica particles with organic groups is difficult since only the surface functionalization is possible for certain groups (silanol groups).[2]

Due to the limitations of the functional groups using the above method, another approach has been developed involving the co-condensation of silane precursors.[2] This includes the Stöber method of synthesis, but involves tetraethoxy silane (TEOS) and organotrialkoxysilane precursors. These organotrialkoxysilane precursors have the empirical formula $RSi(OR')_3$, where R represents methyl, phenyl, octyl, aminopropyl, and mercaptopropyl and R′ represents methyl or ethyl.[9,11-16] However, it was reported that the particles formed by this method ranged from 0.4 – 2.0 µm, which constitutes a very large range of particle size.[2]

Another group of researchers have reported a route for the preparation of silsesquioxanes from a modified Stöber sol-gel method, which involves a sodium silicate solution for the enhancement of the silsesquioxane nanoparticles in a size range 60-180

nm.[2] It was also reported that the size of the particles was dependent on the reaction time, concentration of sodium silicate, organoalkoxy silane precursors, ammonia and water.[2] A non-hydrolytic sol-gel route was also reported by the same group of researchers where they have used dimethyl sulfoxide as the solvent to prepare silsesquioxanes.[17-19]

All the above methods used to synthesize silsesquioxanes are based on an emulsion polymerization technique which involved the use of catalyst, surfactant as an emulsifier and a strong base. These methods resulted in silsesquioxane particles of size ranging from nanometers to micrometers, and had difficulties in controlling the size and morphology of the particles.

The most effective and successful method used to prepare silsesquioxanes has proven to be the hydrolytic condensation (base-catalysed direct hydrolysis and condensation) method of organotrialkoxy silanes.[20] Since these are very reactive, the reaction is carried out in organic solvents in the presence of an acid or a base. The yield and structure of the SSQ's depend on different conditions like reaction time, reaction conditions such as concentration of the monomers, solvent, and functional groups and also the solubility of the SSQ's formed.[21-23]

Several efforts have been made for successful preparation of SSQ's by the hydrolytic condensation method, and various studies were proposed for tuning the sizes, structures, spatial assembly of SSQ's, and functionalities in the silica core by elevating the reaction conditions.[1] Bronstein et al. reported a synthesis by hydrolytic condensation of N-(6-aminohexyl)aminopropyltrimethoxy silane resulting in 30-50 nm spherical SSQ nanoparticles.[24]. By changing the initial conditions of the reaction, they have reported success in preparing particles with controlled size from 30-250 nm.

Until now, there have been no reports on the preparation of benzyl chloride silsesquioxane particles synthesized by a hydrolysis and condensation process, nor the preparation of binary reactive groups of benzyl chloride and amine silsesquioxane particles synthesized by a hydrolysis and co-condensation process. The research described in this thesis describes the development of a versatile method to produce benzyl chloride and amine functionalized silsesquioxane particles in wide size ranges from nanometer scale to micrometer scale.

2.2 Colloidal self-assembly

Colloidal self-assembly is one of the strategies for preparing ordered characteristic patterns of particles. Colloids are molecules or particles which are evenly dispersed in an aqueous medium. Self-assembly is the phenomenon in which the dispersed particles arrange themselves either directly via interactions between the particles or indirectly by applying external stimuli. The silica colloids or spheres which can self-assemble into characteristic patterns ranging in size from nanometers to micrometers. These shapes and patterns of self-assemblies depend on the technique and the substrates used. These colloidal crystals have wide applications in electronic devices, as templates for fabrication, as photonic crystals, etc.[6]

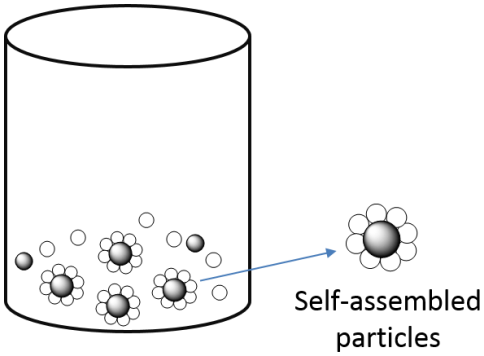

Figure 2.2: Representation of colloidal self-assembly of particles in an aqueous medium

2.2.1 Principles involved in colloidal self-assemblies

Colloidal nanospheres self-assemble via interactions such as van der Waals forces, steric repulsions, and coulombic repulsions.[6] Most self-assemblies occur due to these interactions, however these interactions can be elevated by external stimuli and ordered patterns can be produced. Some different techniques used to self-assemble colloids are:

1. Self-assembly at the interface,
2. Self-assembly during solvent evaporation,
3. Self-assembly by an electric field,
4. Self-assembly by spin coating.

1. Self-assembly at the interface

Self-assemblies of colloids are widely observed at air/water interfaces.[25] The basic principle involved is the binding strength of colloidal particles to liquid interfaces for the formation of an emulsion.[26] The particle interactions with the interface depends on the functionalities of the particles. An electric double layer is formed due to the charge on the functional groups on the surface of the particles to keep the particles at the interface, at

the same time, if there was a same type of charge, this would repel the particle at the interface.[26] An example of a liquid interface due to a charge effect is the hydroxyl ion adsorption at the oil/water interface which charges the interface.[26] In a typical procedure of self-assembly at the interface, the colloids are driven towards the oil/water interface from a water phase and due to their change (lowering) in the interfacial energy, they self-assemble at that particular interface.[26] After the formation of self-assembled colloidal crystals at the liquid interface, they can be transferred onto different substrates for various applications.

2. Self-assembly during solvent evaporation

Self-assembly during solvent evaporation is similar to the drop cast technique. The techniques involved here is based on the observation that when a drop of the colloidal suspension is placed on a planar substrate, self-assemblies are observed on the substrate after evaporation of the solvent.[6] It was reported that the assembly of the colloidal crystals was initiated in the drop when the thickness of the solvent was approximately equal to the diameter of the colloid.[27] The patterns or orders of self-assemblies can be controlled by controlling the rate of solvent evaporation and the angle of the substrate.[28]

3. Self-assembly in electric field

The process involved in this type of self-assembly is based on the observation that when a colloidal suspension is placed in between two electrodes and an electric field is applied, the colloids tend to move towards the electrodes due to their charge properties and the colloids self-assemble are formed at the surface of the electrodes.[6] The movement of the colloids from the suspension towards the surface of the electrodes is driven by the

applied voltage and the self-assembly of the colloids at the surface is induced by the applied electric field. By changing the applied electric field, the patterns of the assembly vary and by increasing the attractive force between the colloids and the electrodes the colloids can be permanently attached to the electrodes.[29-31]

4. Self-assembly during spin-coating

The spin coating technique is the most widely used method, and is known as a fast and reproducible method for formation of self-assembled colloids. The spin coating technique is the method most utilized to produce thin films known for its uniform assembly during semiconductor fabrication.[32-36] In this technique, the colloids are deposited over a flat substrate and rotated at a high spin rate, so that the colloids are dried and packed on the substrate. The thickness and the quality of the colloidal crystals vary depending on the spin speed, concentration of the colloidal suspension, the charge difference between the substrate and the colloids, and also on the nature of the substrate.[6]

CHAPTER 3

RESULTS AND DISCUSSIONS

3.1. Overview

The Stöber method which utilizes a versatile sol-gel route was optimized in the synthesis of all the silsesquioxane particles described in this thesis. My research goal was to prepare benzyl chloride SSQ particles, benzyl chloride-amine SSQ particles, amine functionalized SSQ particles by using a modified Stöber method. The methods developed here can be adapted to make different ligand functionalized SSQ particles with controlled size by varying the concentrations of the base, silane concentration, and the volume of anhydrous ethanol. Self-assemblies of these particles were also studied by utilizing dipole-dipole interactions with different polymer substrates. Polystyrene and polyvinylpyrrolidone (PVP) were used as two different polymer layers to study the particle-polymer interactions and morphology of the resulting self-assemblies. The effect of particle concentration on the morphology of self-assemblies were also studied by varying the particle concentration from lowest to highest weight to volume ratio.

3.2. Synthesis, morphology and characterization of benzyl chloride silsesquioxane (BC-SSQ) particles

3.2.1 Synthesis and characterization of BC-SSQ particles

As depicted in Scheme 3.1, BC-SSQ particles were synthesised by the Stöber method using base catalysed hydrolysis followed by condensation starting from the silane precursor of benzylchloride trimethoxy silane. The particle size and morphology were optimized by varying the base concentration and the volume of ethanol. After the reaction

time of 18 hours, particles were isolated by centrifugation and repeated washing with ethanol followed by water to obtain particles as a white solid. Depending on the base concentration and the volume of the solvent, we observed the variation in particle size, morphology, and yield of the product as summarized in Table 4.1. The silsesquioxane particles obtained in this manner were further characterized by Fourier transform infrared spectroscopy (FTIR) and elemental analysis. In the IR spectrum (Figure 3.1), the Si-O-Si stretching frequency was observed at 1123-1019 cm^{-1} and Si-C stretching appeared at 1306-1262 cm^{-1} which confirm the existence of a siloxane network. The stretching frequency at 1605 cm^{-1} corresponds to the aromatic C=C stretching of the benzyl chloride unit. The alkyl C-H stretching was observed in the frequency range of 3022-2990 cm^{-1}. The signals in the range of 832 to 641 cm^{-1} confirms the presence of aromatic rings. The elemental analysis showed the product had 43.8% carbon and 3.1% hydrogen which was in agreement with the calculated data (C 43.3% and H 3.4) with an empirical formula of $C_7H_7ClSiO_{2.5}$. This formula is consistent with incomplete polymerization with Si-OH chain end groups not fully condensed to $SiO_{1.5}$

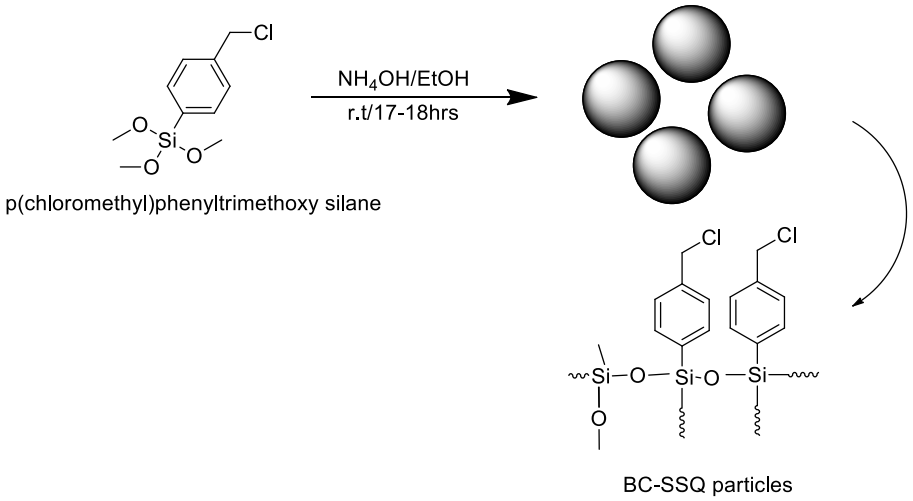

Scheme 3.1: Schematic representation of synthesis of BC-SSQ particles using Stöber method

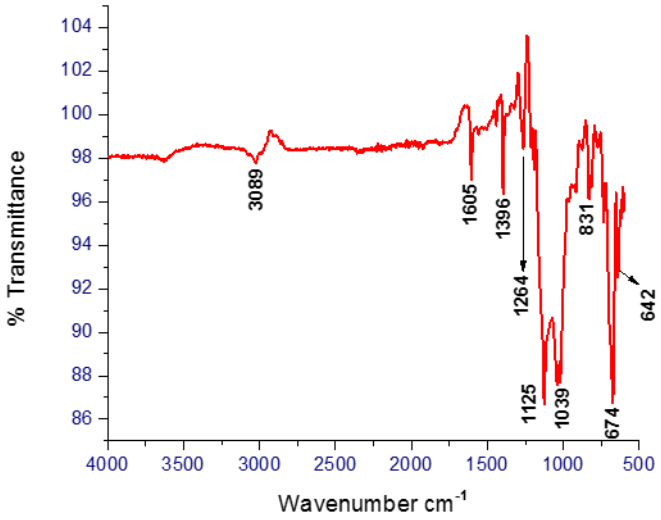

Figure 3.1: FTIR spectrum of BC-SSQ particles

Thermal stability was also studied using thermogravimetric analysis (Figure A-1). The sample exhibits a two-step degradation. The sample exhibits initial weight loss of

2.00% with a slope up to the temperature of 303 ^{0}C. The small weight loss observed here may be due to moisture in the sample. With the next degradation step weight loss of 23.95% took place from 303 ^{0}C to 465 ^{0}C, confirming the partial weight loss from benzyl groups. At 465 ^{0}C, the second step degradation was observed with a weight loss of 10.64% corresponding to the complete degradation of organic content. A total weight loss of 34.59% was observed which corresponds to the total organic content, which is lower than the total weight of the organic content obtained from elemental analysis. From 668 ^{0}C to 800 ^{0}C, the degradation weight loss of 1.32% corresponds to the loss of the siloxane network.

3.2.2 Morphology of BC-SSQ particles

The reaction conditions were optimized and evaluated for the reproducibility of experimental conditions by running different trial reactions. To study the effect of base concentration and volume of ethanol on the morphology of particles, SSQ were synthesized with variations in base concentration and volume of ethanol. The morphology of the particles with changes in the base concentration were characterized using TEM and SEM and summarized in Table 3.1.

Table 3.1: Experimental conditions and morphologies of BC-SSQ particles

Trial #	Benzyl chloride trimethoxy silane	Ammonium hydroxide (28%) (mL)	Anhydrous ethanol (200 proof) (mL)	Yield (%)	Size (μm)
1	1.8 mL (8.16 mmol)	1 (7.26 mmol)	10	94.59%	~2-3 μm (round and spherical)
2	1.8 mL (8.16 mmol)	0.5 (3.63 mmol)	10	87.74%	9-10 μm (round but contains junk around the particles)
3	1.8 mL (8.16 mmol)	0.25 (1.81 mmol)	10	62.24%	Polymerized
4	1.8 mL (8.16 mmol)	2 (14.52 mmol)	10	95.93%	Polymerized
5	1.8 mL (8.16 mmol)	3 (21.78 mmol)	10	82.24%	Polymerized
6	1.8 mL (8.16 mmol)	4 (29.04 mmol)	10	81.5%	Polymerized
7	1.8 mL (8.16 mmol)	1 (7.26 mmol)	20	82.66%	~0.8 μm and ~2 μm (round and spherical)
8	1.8 mL (8.16	1 (7.26 mmol)	30	82.22%	2-3 μm (round

	mmol)				and spherical)
9	1.8 mL (8.16 mmol)	1 (7.26 mmol)	40	78.14%	2-3 µm (round and spherical)

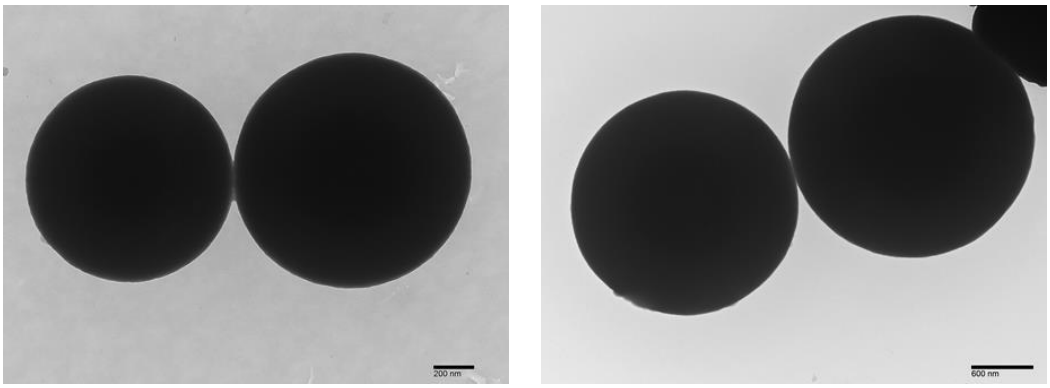

Figure 3.2 TEM images BC-SSQ particles, Trial 1

With the optimized conditions of 8.16 mmol benzyl chloride, 7.26 mmol of base, and 10 mL of ethanol, 10 mL (trial 1, Table 3.1), particles with an average size of 2-3 µm were reproducibly prepared. The resulted particles were spherical in shape as revealed by TEM images (Figure 3.2). When the amount of base decreased to 3.6 mmol (trial 2), there was a significant increase of particle size to 9-10 µm (Figure 3.3). However, this trial could not be reproduced and unorganised polymerized structures were observed (Table A-1). When the amount of base was decreased to half fold to 1.81 mmol (trial 3), similar polymerized nanostructures were observed under TEM as shown in Figure 3.4. The polymerized nanostructures formed can be due to the lack of nucleation sites to initiate the particle formation. Similar polymerized nanostructures/aggregates were observed with the amount of base increased by four fold from 7.26 mmol (trial 4, 5 and 6). The images of these polymerized structures are depicted in Figure 3.5, 3.6, and 3.7.

This can be attributed to spontaneous hydrolysis of silane precursor upon high base concentration.

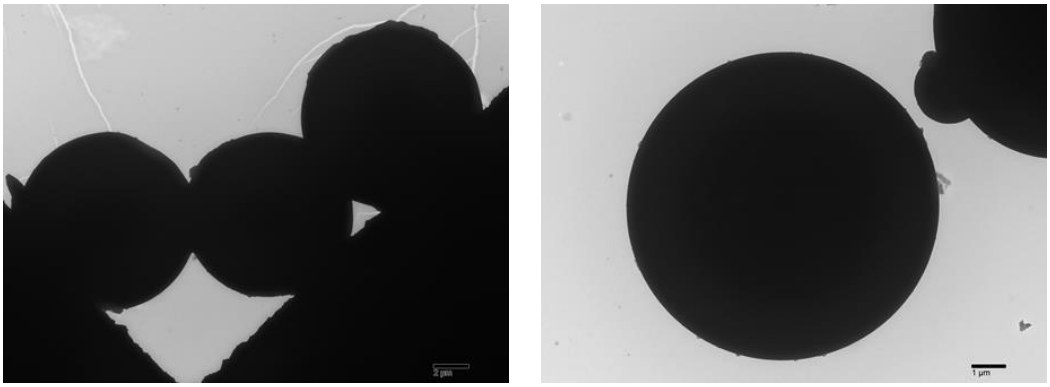

Figure 3.3 TEM images BC-SSQ particles, Trial 2

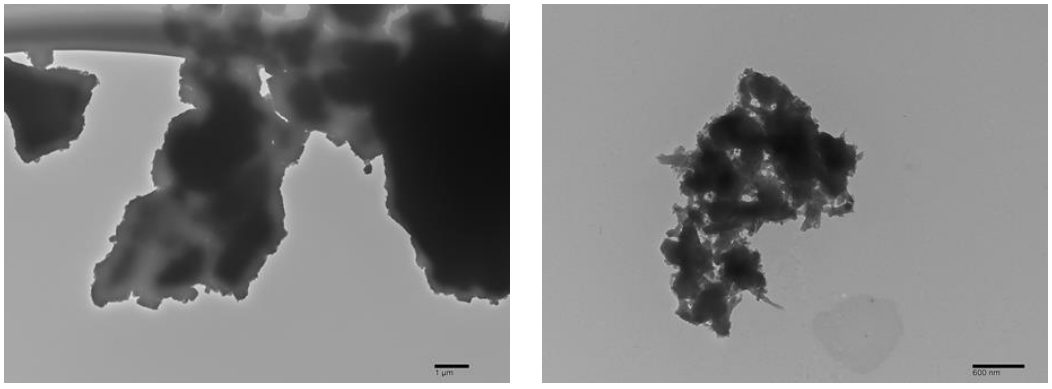

Figure 3.4 TEM images BC-SSQ particles, Trial 3

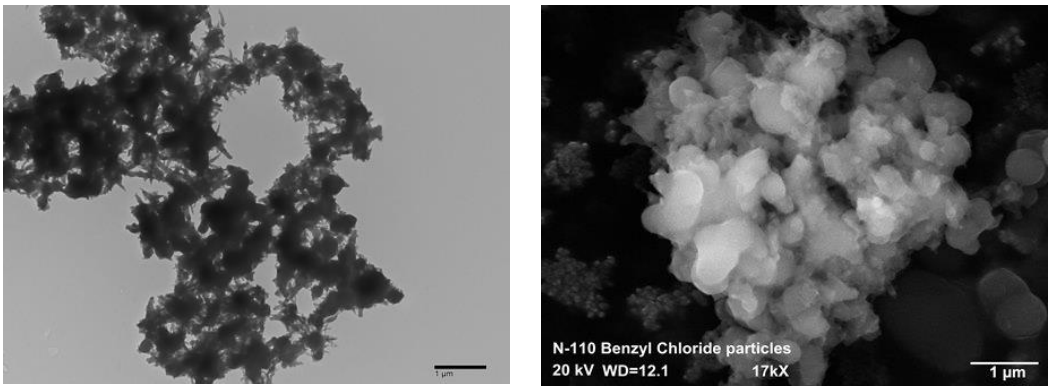

Figure 3.5: TEM and SEM images of BC-SSQ particles, Trial 4

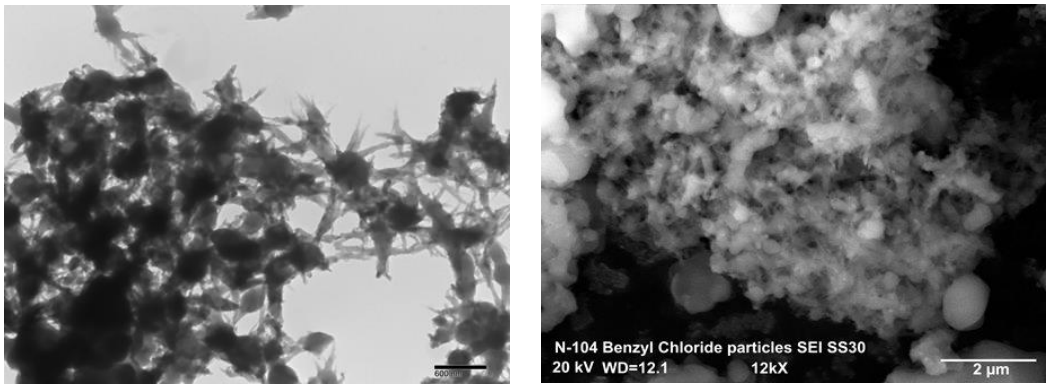

Figure 3.6: TEM and SEM images of BC-SSQ particles, Trial 5

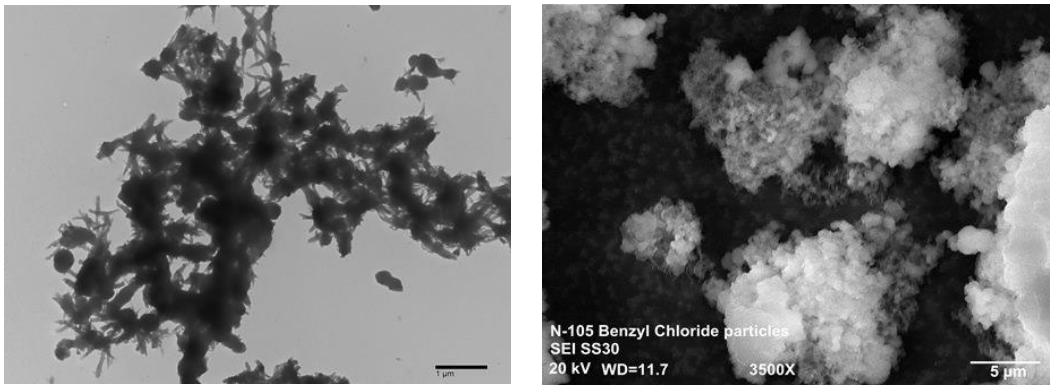

Figure 3.7: TEM and SEM images of BC-SSQ particles, Trial 6

With increasing solvent volume, although there was no effect on particle size or the morphology, there was a distinct effect on the particle size distribution. When the volume of ethanol was increased to 20 mL (trial 7) while keeping the amounts of benzyl chloride and base concentration at 8.16 mmol and 7.26 mmol respectively, the particle size range was from 800 nm to 2 µm. (Figure 3.8). Doubling of solvent volume to 40 mL (trial 8 and 9, Table 3.1) resulted in particles with a size ranging from 2 - 3 µm (Figure 3.9). These results clearly show that there is no effect of solvent volume on either particle size or morphology which is governed by the amount of base.

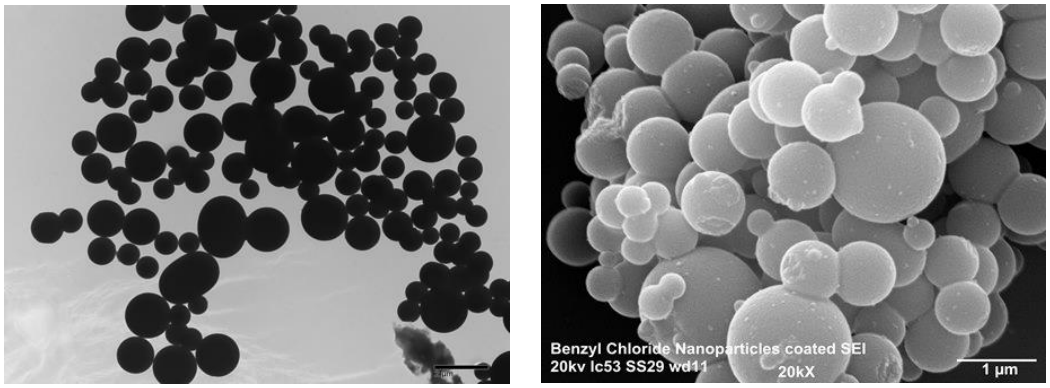

Figure 3.8: TEM and SEM images of BC-SSQ particles, Trial 7

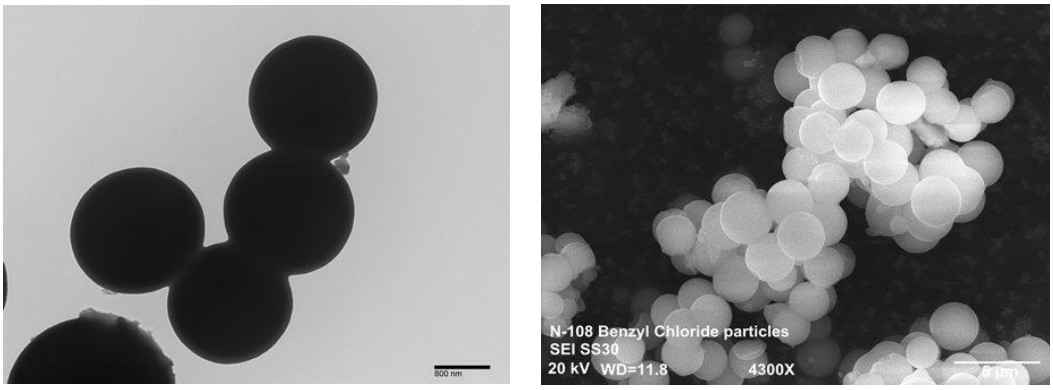

Figure 3.9: TEM and SEM images of BC-SSQ particles, Trial 8 and 9

3.2.3 Synthesis and characterization of anthracene-functionalized BC-SSQ particle

As depicted in Scheme 3.2, BC-SSQ particles were functionalized with anthracene methanol by Williamson ether synthesis at room temperature for approximately 18 hours to a yield pale yellow solid. The pale yellow solid obtained was isolated by repeated centrifugation by re-dispersing the solid in ethanol and water. The silsesquioxane particles obtained were further characterized by FTIR and elemental analysis. In the IR spectrum (Figure 3.10), the Si-O-Si stretching frequency appeared at 1124-1019 cm^{-1} and the Si-C stretching frequency at 1306-1262 cm^{-1}, confirming the presence of a siloxane network after functionalizing the BC-SSQ particles. The stretching

frequency at 1605 cm^{-1} corresponds to the aromatic C=C stretching. The alkyl C-H stretching was observed at a frequency 3026-2990 cm^{-1}.

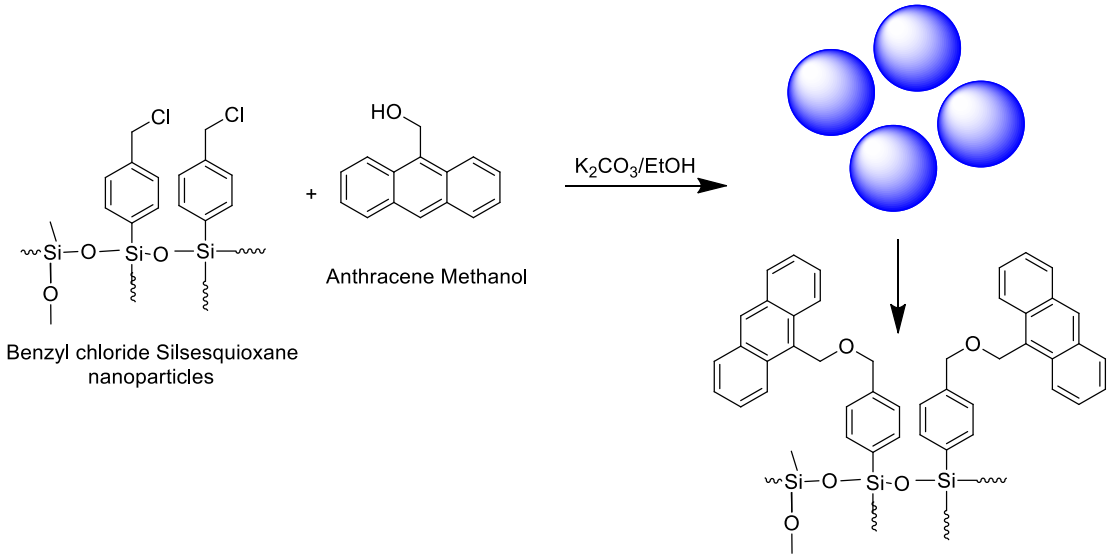

Scheme 3.2: Schematic representation of functionalization of BC-SSQ particles with anthracene methanol

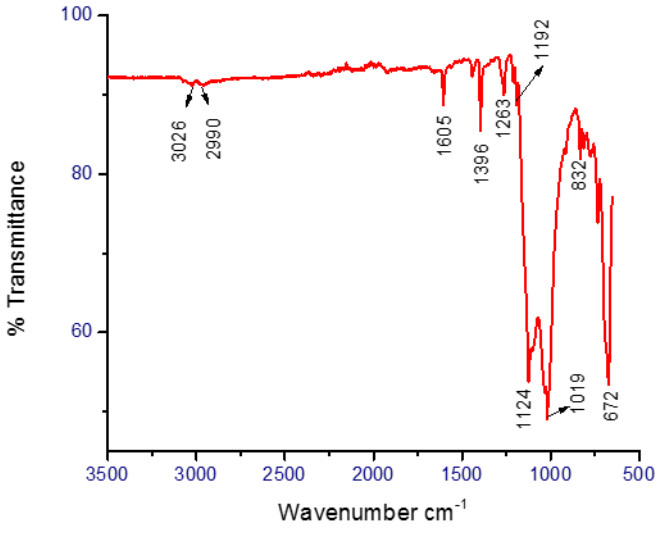

Figure 3.10: FTIR spectrum of anthracene functionalized BC-SSQ particles

Thermal analysis of the anthracene functionalized BC-SSQ particles was also studied using thermogravimetric analysis (Figure A-2). The sample exhibits two steps degradation process. The sample exhibits an initial weight loss of 2.00% with a slope up to the temperature of 295 ^{0}C. The small weight loss observed here was may be due to moisture of the sample. With the next degradation step a weight loss of 18.22% took place from 295 ^{0}C to 458 ^{0}C, confirming the particle weight loss of benzyl groups and anthracene units. At 458 ^{0}C, the second step degradation was observed with a weight loss of 15.67% corresponding to the complete degradation of organic content. A total weight loss of 34% was observed which corresponds to the total organic content which is lower than the total weight of organic content obtained from elemental analysis. A weight loss of 1.24% from 664 ^{0}C to 800 ^{0}C corresponds to the partial degradation of the siloxane network.

3.2.4 Morphology of anthracene-functionalized BC-SSQ particles

The morphology of anthracene functionalized BC-SSQ particles were studied using TEM and a fluorescence optical microscope. The morphology and size of the particles remained the same upon post functionalization. The TEM images of post functionalized particles confirmed the size and shape of the particles (Figure 3.11). A fluorescence optical microscope was used to visualize these particles. The anthracene functionalized particles were dispersed in nanopure water and then dropped on a glass slide and were smeared with a cover slip. The particles visualized using a DAPI filter at 100X magnification confirms successful incorporation of the blue fluorescence tag onto the particle periphery and the core. (Figure 3.12).

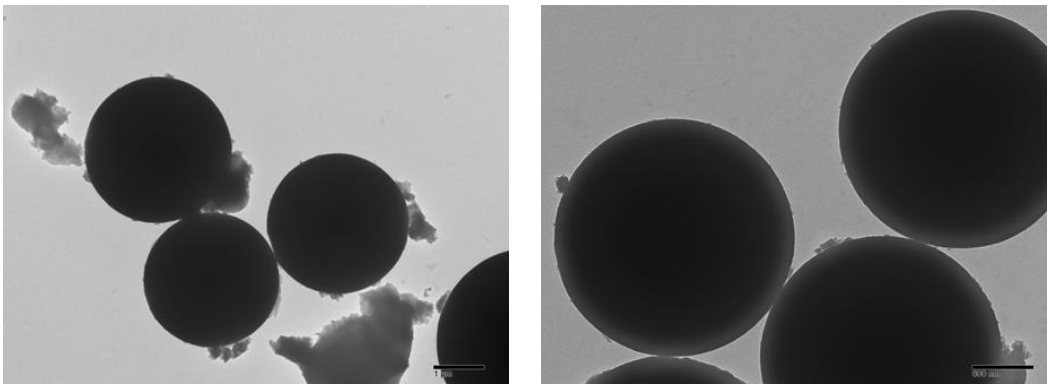

Figure 3.11: TEM images of anthracene functionalized BC-SSQ particles

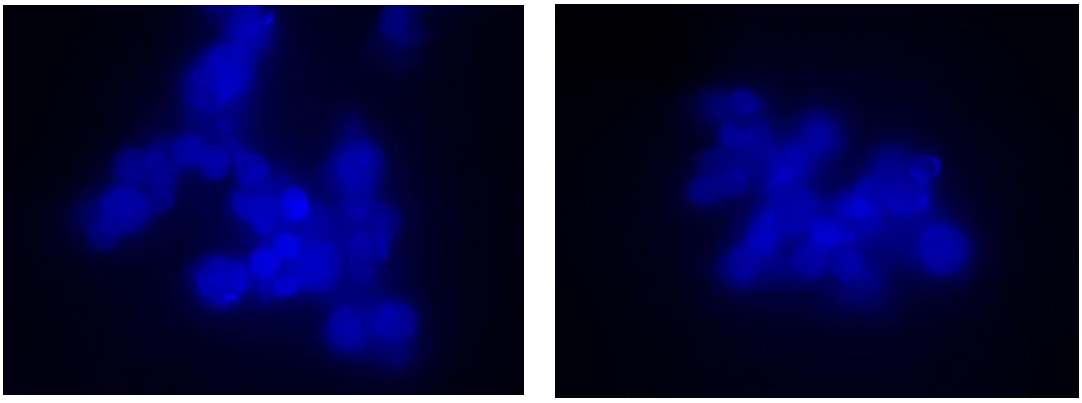

Figure 3.12: Fluorescence optical microscope images of anthracene functionalized BC-SSQ particles (DAPI filter)

3.2.5 Photophysical properties

The photophysical properties of anthracene functionalized BC-SSQ particles were studied in ethanol solution. As shown in Figure 3.13(a) a set of distinct absorption peaks were observed. Three distinct vibrational transitions at wavelengths of 347 nm, 365 nm and 384 nm are characteristic of anthracene absorbance. The absorption peaks ranging from 347-384 nm confirms the presence of the anthracene moiety attached to BC-SSQ particles. The fluorescence emission spectra in ethanol solution was obtained and is shown in Figure 3.13(b). The emission spectrum shows the maximum emission at 413

nm upon excitation at 340 nm. The three distinct vibronic bands at 392 nm, 414 nm and 439 nm gives the clear evidence of the attachment of anthracene moieties.

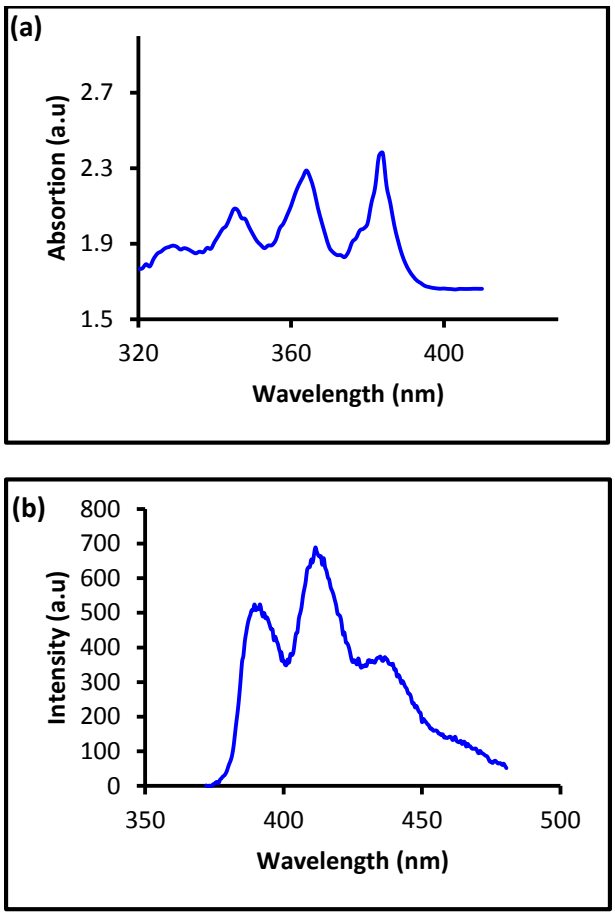

Figure 3.13: (a) UV-Vis absorption spectrum; (b) Fluorescence emission spectrum, in ethanol solution (excited at 340 nm)

3.3. Synthesis, morphology and characterization of benzyl chloride-amine silsesquioxane (BC-amine-SSQ) particles

3.3.1 Synthesis and characterization of BC-amine-SSQ particles

As depicted in Scheme 3.3, BC-amine-SSQ particles were synthesized by the Stöber method by base catalysed hydrolysis followed by co-condensation starting from

the silane precursor of benzyl chloride trimethoxy silane and 3-aminopropyl trimethoxy silane (3-APT). The particle size and morphology were optimized by varying the base concentration and volume of ethanol. After reaction for 18 hours, particles were isolated by centrifugation and repeated washing with ethanol followed by water to obtain particles as a white solid. Depending on the base concentration and the volume of the solvent, we observed a variation in particle size, morphology, and yield of the product as summarized in Table 3.2. Particles obtained in this manner were further characterized by FTIR and elemental analysis. In the IR spectrum (Figure 3.14), the Si-O-Si stretching frequency appeared in the range of 1127-1020 cm^{-1} and Si-C stretching frequency in the range 1397-1264 cm^{-1} confirming the existence of a siloxane network. The stretching frequency at 1605 cm^{-1} shows the aromatic C=C stretching from benzyl chloride. Alkyl C-H stretching was also observed at a frequency 2997 cm^{-1}. The stretching range from 832 to 641 cm^{-1} confirms the presence of aromatic rings. We do not observe the N-H stretching of the amine functionality from 3-APT in the IR spectrum. This may be due to the partial incorporation of 3-APT during the co-condensation. The elemental analysis confirmed the total carbon content of 39.4.0% with 3.8% hydrogen and 0.8% nitrogen which was in agreement with the theoretical elemental analysis (C 39.4%, H 4.96% and N 4.5%). The reduced nitrogen content provides further evidences for partial hydrolysis and co-condensation of 3-APT into the siloxane network.

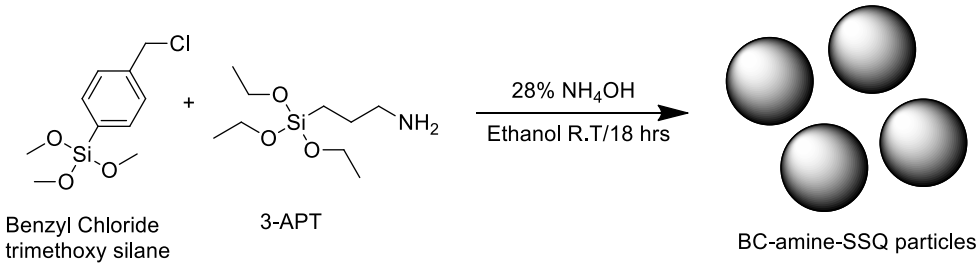

Scheme 3.3: Schematic representation for the synthesis of BC-amine-SSQ particles

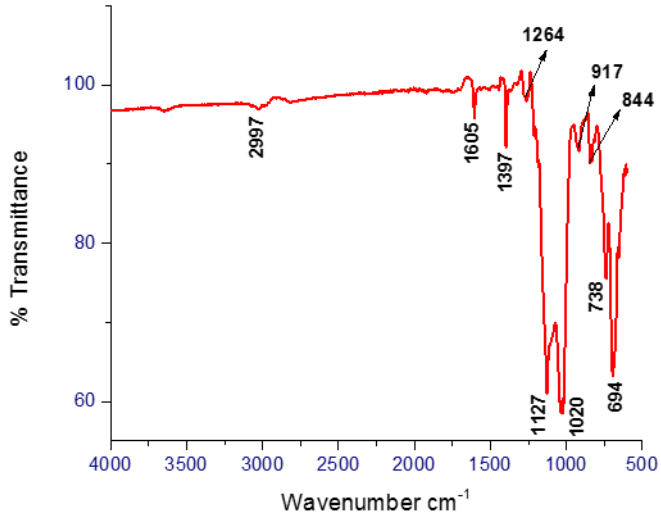

Figure 3.14: FTIR spectrum of BC-amine SSQ particles

Thermal stability of the BC-amine SSQ particles was also studied using thermogravimetric analysis (Figure A-3). The sample exhibits a two-step degradation process. The sample exhibits initial weight loss of 2.5% with a slope up to the temperature of 160 ^{0}C. With the next degradation step a weight loss of 23.43% took place from 160 ^{0}C to 428 ^{0}C confirming the partial weight loss of benzyl groups and organic alkyl content. At 428 ^{0}C, a second step degradation was observed with a weight loss of

18.50% corresponding to complete degradation of remaining organic content. A total weight loss of 41.93% was observed corresponding to the total organic content, which is similar to the total weight of organic content obtained from the elemental analysis. From 663 ^{0}C to 800 ^{0}C the degradation corresponds to the loss of siloxane network with a weight loss of 1.40%.

3.3.2 Morphology of BC-amine-SSQ particles

The reaction conditions were optimized and were checked for their reproducibility of experimental conditions by running different trial reactions. The reaction conditions were altered to study the effect of base concentration and volume of ethanol on the morphology of particles. The morphology of the particles with changes in the base concentration were characterized using TEM and SEM and summarized in Table 3.2.

Table 3.2: Experimental conditions and morphologies of BC-amine-SSQ particles

Trial #	Benzyl chloride trimethoxy silane (mL)	3-APT silane (mL)	Ammonium hydroxide (mL)	Anhydrous ethanol (mL)	Yield	Size
1	1 (4.53 mmol)	2 (8.54 mmol)	3.5 (25.41 mmol)	65	43.18%	~1.7-1.9 µm (round and spherical)
2	1 (4.53 mmol)	2 (8.54 mmol)	3.5 (25.41 mmol)	130	23.2%	~1.5-1.7 µm (round and spherical)
3	1 (4.53 mmol)	2 (8.54 mmol)	7 (50.82 mmol)	65	21.55%	~1.2-1.5 µm (round and spherical)
4	1 (4.53 mmol)	2 (8.54 mmol)	1.75 (12.70 mmol)	65	21.03%	~2-2.1µm (round and spherical)

With the optimized conditions of 4.53 mmol benzyl chloride silane, 8.53 mmol of 3-aminopropyl trimethoxy silane and 25.41 mmol of base and a volume of 65 mL ethanol (Trial 1, Table 3.2), particles with an average size of 1.7-1.9 µm were able to be prepared

repeatedly. The resulted particles were spherical in shape as revealed by the TEM and SEM images (Figure 3.15). When the volume of the solvent was doubled by twofold to 130 mL, no change in the size of the particles were observed which clearly indicates that there is no effect of solvent volume on the size and morphology of the particles (Figure 3.16).

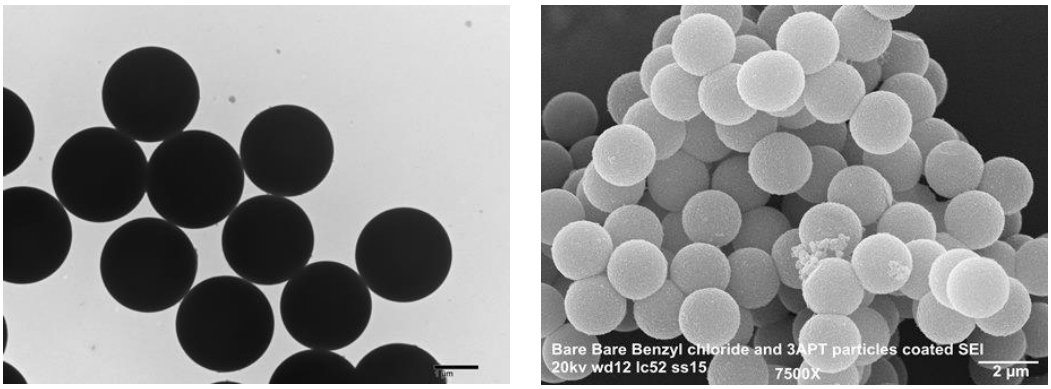

Figure 3.15: TEM and SEM images of BC-amine-SSQ particles, Trial 1

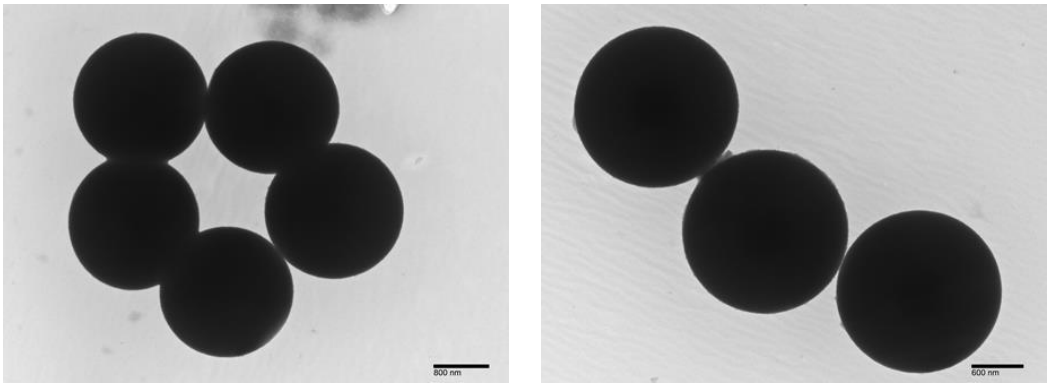

Figure 3.16: TEM images of BC-amine-SSQ particles, Trial 2

When the amount of the base was doubled to twofold to 50.82 mmol (trial 3, Table 3.2), the particle size range was from 1.2-1.4 µm (Figure 3.17). When the amount of the base was decreased to half fold to 12.70 mmol (trial 4, Table 3.2), particle size range was from 2.1 µm (Figure 3.18). These results clearly evidence that while there is

no effect of solvent volume on the particles, the size and morphology of the particles do depend on the base concentration. It was also observed that the particle yield was low and this can be attributed due to incomplete incorporation of amine functionality with benzyl chloride silane.

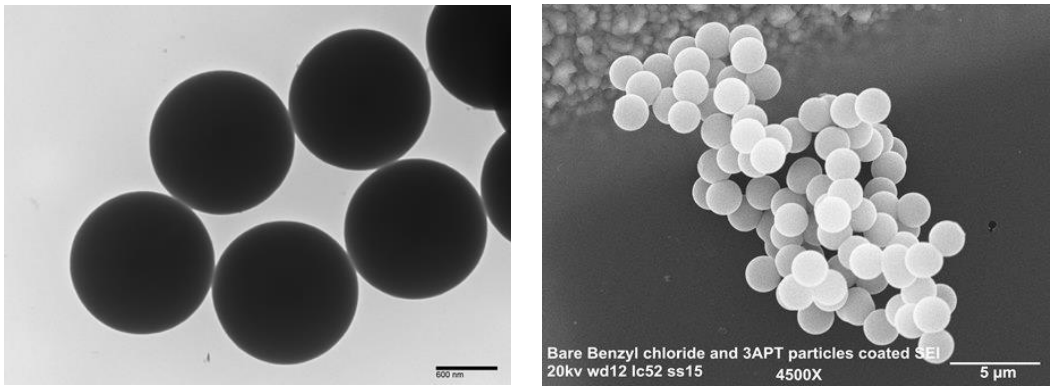

Figure 3.17: TEM and SEM images of BC-amine-SSQ particles, Trial 3

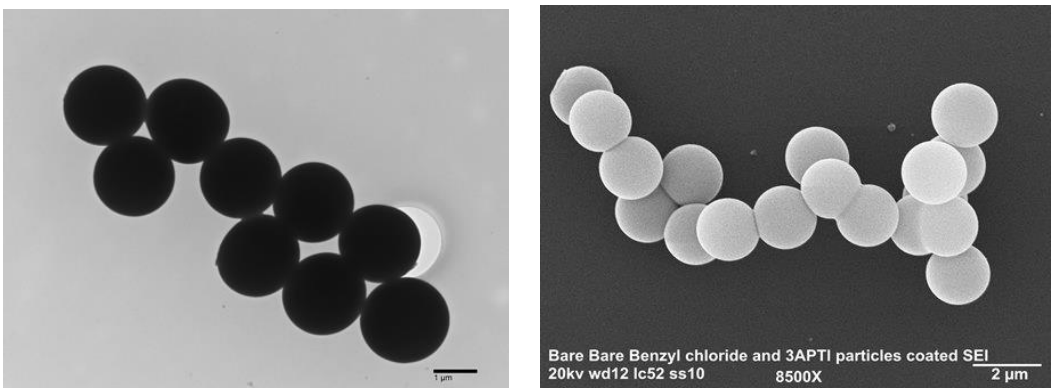

Figure 3.18: TEM and SEM images of BC-amine-SSQ particles, Trial 4

3.3.3 Synthesis and characterization of anthracene and rhodamine-B functionalized BC-amine SSQ particles

As depicted in scheme 3.4, BC-amine-SSQ particles were multi-functionalized with anthracene methanol and rhodamine B by a two-step process. First, BC-amine-SSQ

particles were functionalized with anthracene methanol by a Williamson ether synthesis at room temperature over-night to yield a pale yellow solid. These pale yellow solid obtained was isolated by repeated centrifugation after re-dispersing the solid in ethanol and water. Dried anthracene functionalized BC-amine-SSQ particles were functionalized with rhodamine B using the well-known method called Steglich esterification method in the presence of dicyclohexylcarbodiimide for approximately 18 hours to yield pink solid. The pink solid obtained was isolated by repeated centrifugation after re-dispersing the solid in ethanol and water and dried under vacuum for 24 hours. The particles obtained in this manner were further characterized by FTIR and elemental analysis. In the IR spectrum (Figure 3.19), the Si-O-Si stretching frequency was observed in the range of 1123-1019 cm^{-1} and the Si-C stretching frequency at 1396-1261 cm^{-1} confirming the presence of a siloxane network after functionalizing the BC-amine-SSQ particles. The stretching frequency at 1606 cm^{-1} shows the aromatic C=C stretching. The alkyl C-H stretching was also observed at a frequency of 2981 cm^{-1}. The stretching frequency at 1442 cm^{-1} indicates the N-C stretching which confirms the coupling of rhodamine-B to the BC-amine-SSQ particles. The stretching range from 832 to 642 cm^{-1} confirms the presence of aromatic rings.

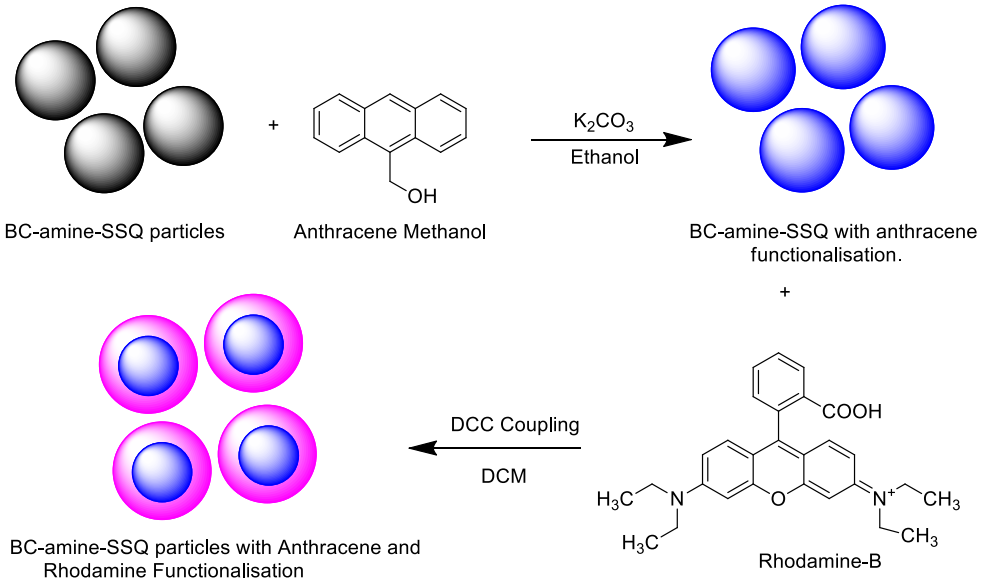

Scheme 3.4: Schematic representation of functionalization of BC-amine-SSQ particles with anthracene and rhodamine-B

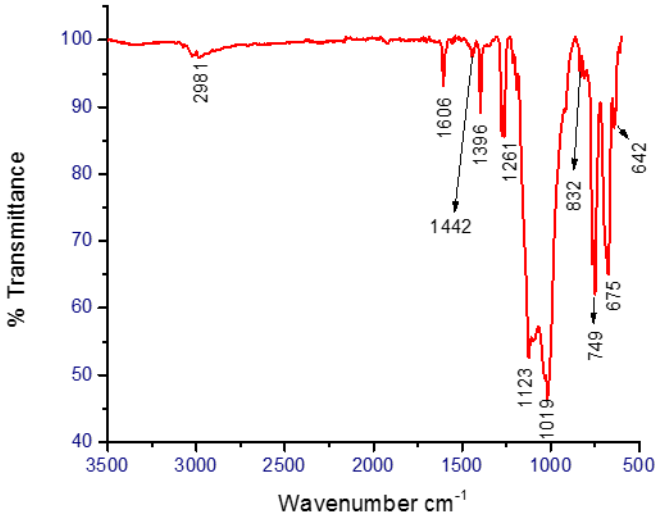

Figure 3.19: FTIR spectrum of anthracene and rhodamine-B functionalized BC-amine SSQ particles

Thermal stability of the anthracene and rhodamine-B functionalized BC-amine SSQ particles was also studied using thermogravimetric analysis (Figure A-4). The sample exhibits a two-step degradation process. The sample exhibits an initial weight loss of 2.00% with a slope up to the temperature of 190 ^{0}C. The small weight loss observed here may be due to the moisture of the sample. With the next degradation step a weight loss of 18.14% took place from 190 ^{0}C to 425 ^{0}C confirming the partial weight loss from the benzyl, alkyl, anthracene and rhodamine groups. At 425 ^{0}C, a second step degradation was observed with a weight loss of 17.97% corresponding to the loss of total organic content. A total weight loss of 36.11% was observed which corresponds to the total organic content, which was lower than the total weight of organic content from the elemental analysis. From 663 ^{0}C to 800 ^{0}C the weight loss of 1.84% corresponds to a degradation of the siloxane network.

3.3.4 Morphology of anthracene and rhodamine-B functionalized BC-amine SSQ particles

The morphology of anthracene and rhodamine functionalized BC-amine-SSQ particles were studied using TEM and SEM. The shape and size of the particles remained same post functionalization. The TEM and SEM images of post functionalized particles confirmed the size and shape of the particles (Figure 3.20). A fluorescence optical microscope was also used to visualize these particles. The anthracene and rhodamine functionalized particles were dispersed in nanopure water and then dropped on a glass slide and were smeared with a cover slip. The particles visualized using a DAPI and rhodamine filter at 100X magnification confirms the covalent attachment of both fluorescent tags onto particles. Under the DAPI filter, particles exhibit blue fluorescence

and under the rhodamine filter particles exhibit red fluorescence. Particles show blue-pink fluorescent colour under both filters (see Figure 3.21).

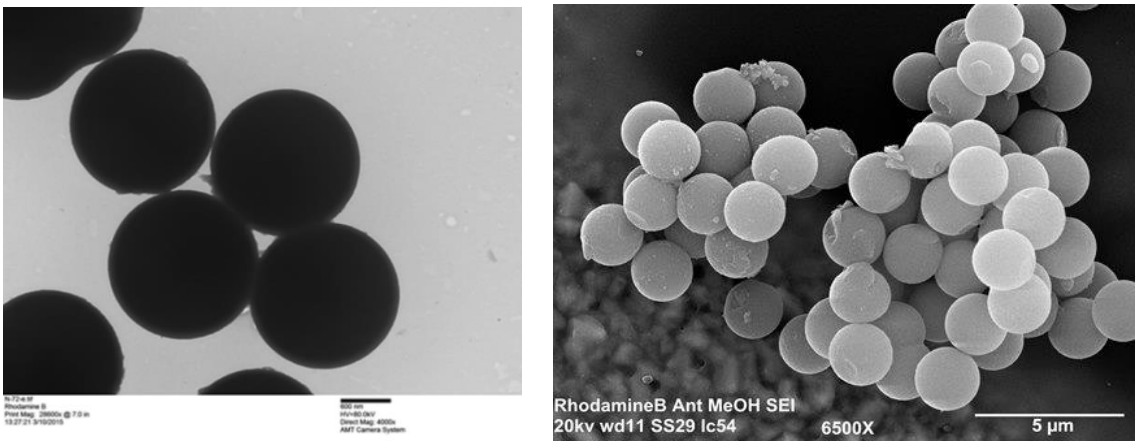

Figure 3.20: TEM and SEM images of anthracene and rhodamine functionalized BC-amine-SSQ particles

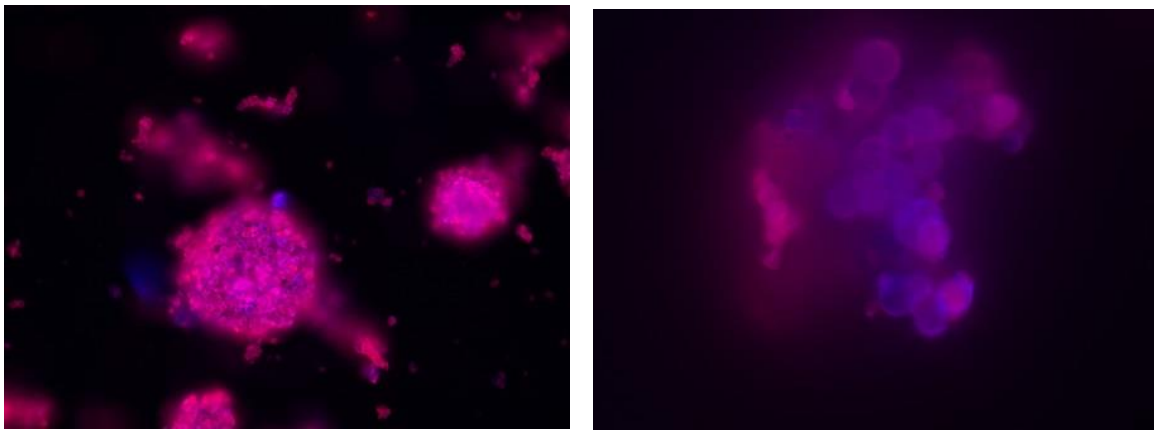

Figure 3.21: Fluorescence optical microscope images of anthracene and rhodamine functionalized BC-SSQ particles (DAPI and rhodamine filter)

3.3.5 Photophysical properties: (Anthracene and rhodamine functionalized BC-amine-SSQ particles)

Photophysical properties of multi-functionalized BC-amine-SSQ particles were obtained in ethanol solution. As shown in Figure 3.22(a) a set of distinct absorption peaks were observed. The distinct vibrational transitions at wavelengths 276-350 nm are the characteristic of anthracene absorbance. The absorption peaks ranging from 276-350 nm confirms the presence of anthracene moiety attached to BC-amine-SSQ particles. Although the absorption spectrum does not exhibit the absorption from rhodamine B, the fluorescence spectrum is well resolved to distinct the emission from both fluorescent tags. The fluorescence emission spectrum in ethanol solution was obtained and is shown in Figure 3.22(b). The emission spectrum shows a maximum emission at 410 nm when excited at 340 nm. The three distinct vibronic bands at 392 nm, 415 nm and 435 nm give us clear evidence of the attachment of anthracene moieties. A single peak at wavelength of 580 nm is characteristic to the emission from rhodamine-B.

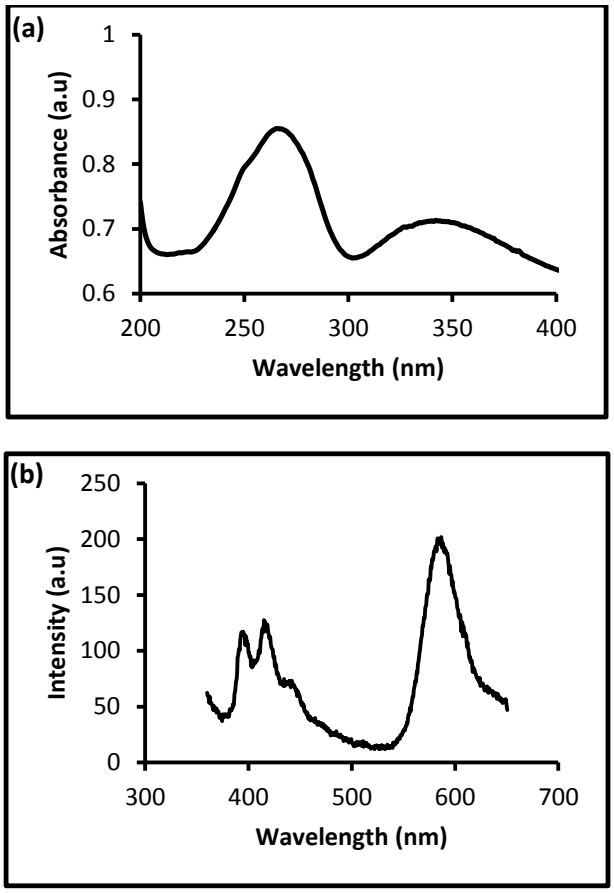

Figure 3.22: (a) UV-Vis absorption spectrum, (b) Fluorescence emission spectrum in ethanol solution (excited at 340 nm)

3.3.6 Synthesis and characterization of rhodamine functionalized BC-amine SSQ particles

As depicted in Scheme 3.5, BC-amine-SSQ particles were functionalized with rhodamine-B via Steglich esterification in the presence of dicyclohexylcarbodiimide for approximately 18 hours to yield a pink solid. The pink solid obtained was isolated by repeated centrifugation after re-dispersing the solid in ethanol and water and dried under vacuum for 24 hours. The silsesquioxane particles obtained in this manner were further characterized by FTIR and elemental analysis. In the IR spectrum (Figure 3.23), the Si-O-

Si stretching was observed in the range of 1124-1020 cm^{-1} and Si-C stretching in the range of 1396-1261 cm^{-1}, confirming the presence of a siloxane network after functionalizing BC-amine-SSQ particles. The stretching frequency at 1605 cm^{-1} shows the aromatic C=C stretching. The alkyl C-H stretching was also observed at a frequency 2988 cm^{-1}. The stretching frequency at 1442 cm^{-1} indicates the N-C stretching which confirms the coupling of rhodamine-B to BC-amine-SSQ particles. The stretching range from 832 to 690 cm^{-1} confirms the presence of aromatic rings.

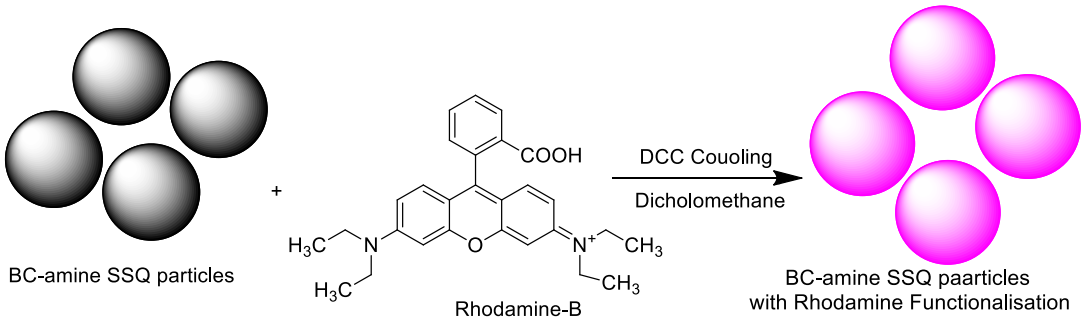

Scheme 3.5: Schematic representation of functionalization of BC-amine-SSQ particles with rhodamine-B

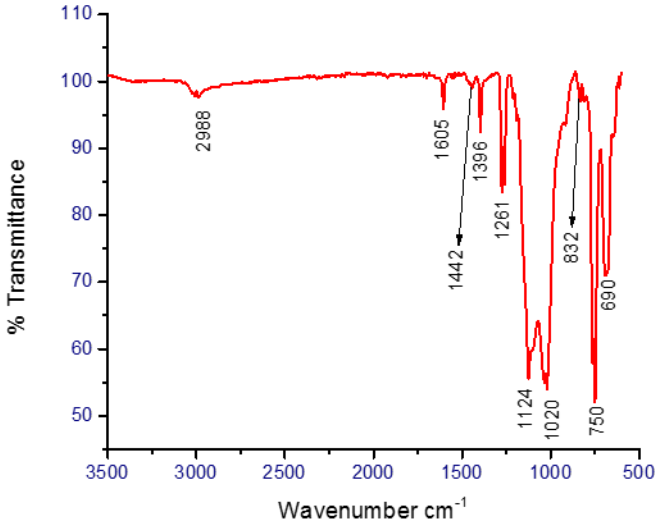

Figure 3.23: FTIR spectrum of rhodamine-B functionalized BC-amine SSQ particles

Thermal stability of rhodamine-B functionalized BC-amine SSQ particles was also studied using thermogravimetric analysis (Figure A-5). The sample exhibits two step degradation process. The sample exhibits an initial weight loss of 2.00% with a slope up to the temperature of 104 ^{0}C. The small weight loss observed here may be due to the moisture of the sample. With the next degradation step a weight loss of 23.74% resulted from 104 ^{0}C to 413 ^{0}C confirming a partial weight loss from benzyl, alkyl, and rhodamine groups. At 413 ^{0}C, a second step degradation was observed with a weight loss of 16.73% corresponding to the loss of total organic content. A total weight loss of 40.47% was observed which corresponds to the total organic content, which is lower than the weight of organic content resulted from elemental analysis. From 663 ^{0}C to 800 ^{0}C a weight loss of 1.52% corresponds to degradation of siloxane network.

3.3.7 Morphology of rhodamine functionalized BC-amine SSQ particles

The morphology of rhodamine functionalized BC-amine-SSQ particles was studied using TEM and SEM. The shape and size of the particles remained the same post functionalization. The TEM and SEM images of post-functionalized particles confirmed the size and shape of the particles (Figure 3.24). The successful incorporation of fluorescence functional groups was confirmed using a UV-Vis and Fluorescence spectrometer.

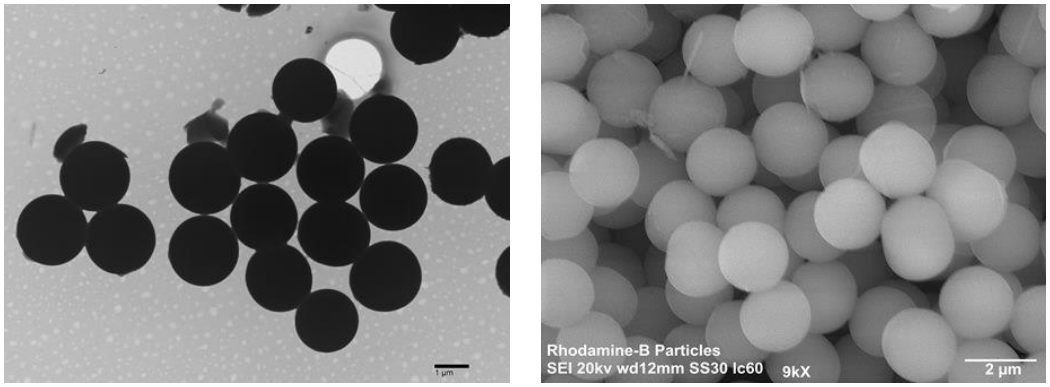

Figure 3.24: TEM and SEM images of rhodamine functionalized BC-amine-SSQ particles

3.3.8 Photophysical properties: (Rhodamine functionalized BC-amine SSQ particles)

The photophysical properties of rhodamine functionalized BC-amine-SSQ particles were studied in ethanol solution. As shown in the Figure 3.25(a), a distinct peak at wavelength 560 nm is characteristic of rhodamine-B absorbance which further confirms the presence of the rhodamine-B moiety attached to the BC-amine-SSQ particles. The Fluorescence emission spectrum (Figure 3.25(b)) clearly shows a vibronic

band at a wavelength of 560 nm when excited at 540 nm, indicating the presence of rhodamine-B.

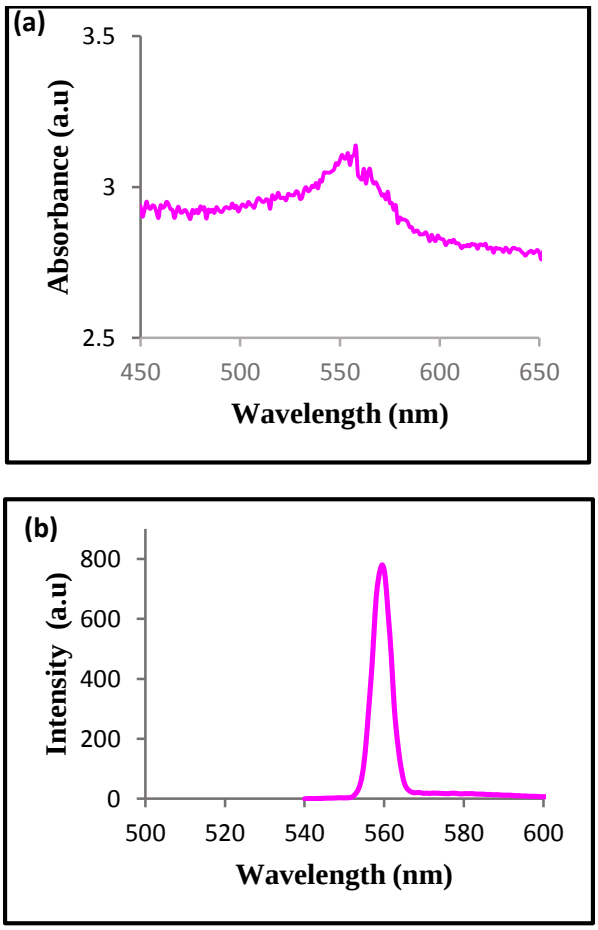

Figure 3.25: (a) UV-Vis absorption spectrum, (b) Fluorescence emission spectrum in ethanol solution (excited at 540 nm)

3.4 Synthesis, morphology and characterization of amine functionalized silsesquioxane (Amine-SSQ) particles

3.4.1 Synthesis and characterization of amine-SSQ particles

As depicted in Scheme 3.6, amine-functionalized SSQ particles were synthesized by the Stöber method upon base catalyzed hydrolysis followed by co-condensation starting from the silane precursors of tetraethoxy silane and 3-APT silane. The particle size and morphology were optimized by varying the base concentration and the volume of ethanol. After the reaction of 18 hours, particles were isolated by centrifugation and repeated washing with ethanol followed by water to obtain the product as a white solid. Depending on the base concentration and the volume of the solvent, we observed a variation in particle size, morphology, and yield of the product as summarized in Table 3.3. The silsesquioxane particles obtained in this manner were further characterized by FTIR and elemental analysis. In the IR spectrum (Figure 3.26), the Si-O-Si stretching frequency at 1044 cm^{-1} confirms the existence of the siloxane network. The slight curve at 3300 cm^{-1} shows us that there was some incorporation of the amine functionality (N-H stretch) to siloxane network.

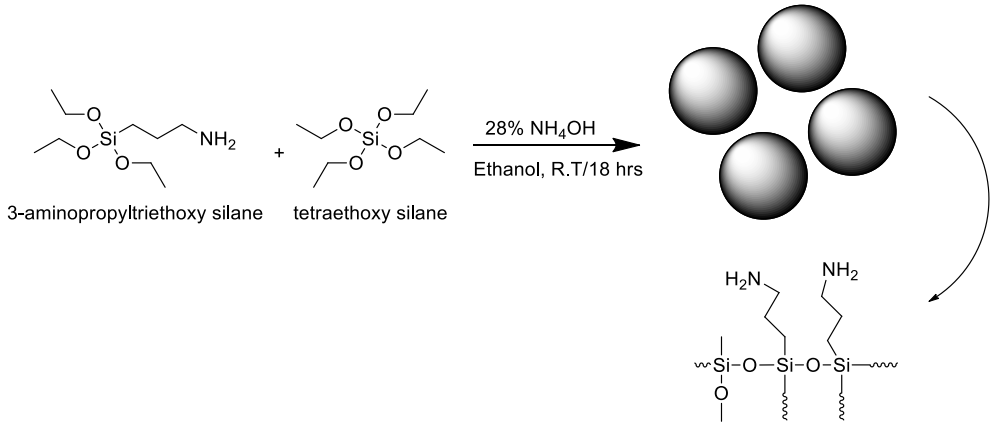

Scheme 3.6: Schematic representation of synthesis of amine-SSQ particles.

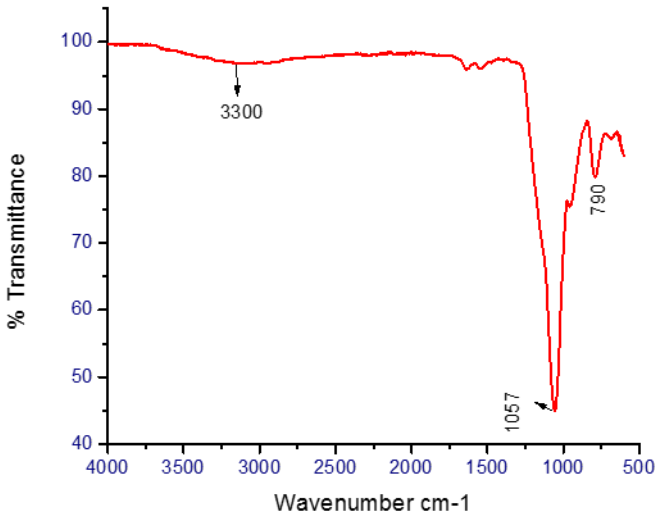

Figure 3.26: FTIR spectrum of amine-SSQ particles

Thermal stability of the amine-SSQ particles was also studied using thermogravimetric analysis (Figure A-6). The sample exhibits a three step degradation process. In the first degradation step a weight loss of 4.68% took place from 102 ^{0}C to 465 ^{0}C confirming partial weight loss from alkyl groups of TEOS and 3-APT. A second degradation step from 465 ^{0}C to 489 ^{0}C with a weight loss of 6.89% was observed

confirming the weight loss of total alkyl content. At 489 ^{0}C the third step degradation with a weight loss of 5.30% confirmed the complete degradation of the organic content. A total of 16.87% weight loss was observed corresponding to the total organic content. From 633 ^{0}C to 800 ^{0}C, the degradation corresponds to the loss of siloxane network with weight loss of 1.2%.

3.4.2 Morphology of amine-SSQ particles

The reaction conditions were optimized and evaluated for the reproducibility of experimental conditions by running different trial reactions. To study the effect of base concentration and volume of ethanol on the morphology of particles, SSQ were synthesized with variations in base concentration and volume of ethanol. The morphology of the particles with changes in the base concentration were characterized using TEM and SEM and are summarized in Table 3.3.

Table 4.3: Experimental conditions and morphologies of amine-SSQ particles

Trial #	Tetraethoxy silane (mL)	3-APT silane (mL)	Ammonium hydroxide (mL)	Anhydrous ethanol (mL)	Yield	Size
1	1 (4.47 mmol)	3 (12.82 mmol)	6 (43.56 mmol)	20	19.2%	~0.400 µm (not perfect spherical)
2	1 (4.47 mmol)	3 (12.82 mmol)	8 (58.08 mmol)	20	18.3%	~0.350 µm (round and spherical)
3	1 (4.47 mmol)	3 (12.82 mmol)	10 (72.60 mmol)	20	25.3%	~0.350 µm (round and spherical)
4	1 (4.47 mmol)	3 (12.82 mmol)	20 (145.20 mmol)	40	11.1%	~0.250-0.3 µm (round and spherical)

With the optimized conditions of 4.47 mmol tetraethoxysilane, 12.82 mmol 3-aminopropyltrimethoxy silane, 43.56 mmol of base and 20 mL ethanol, (trial 1, Table

3.3), particles with average size of ~400 nm were prepared and was able to reproduced. The resulted particles were not perfectly spherical in shape as revealed by TEM images (Figure 3.27). When the amount of the base increased to 58.08 mmol (trial 2), the particle size was 0.350 µm of perfectly spherical shape (Figure 3.28). When the amount of base was increased further to 72.60 mmol (trial 3), there was no effect on the particle size but the particles were more spherical in shape when compared to trial 2 as shown in Figure 3.29. When the amount of the base was increased further to 145.20 mmol, with an increase in the solvent volume to 40 mL as well, keeping TEOS and 3-APT silane concentration at 4.47 mmol and 12.82 mmol respectively (trial 4), a gradual decrease in the particle size to 0.250 µm was observed, which was confirmed by TEM images (Figure 3.30). These results clearly indicate that the particles size and morphology depend on the amount of the base as well as the solvent.

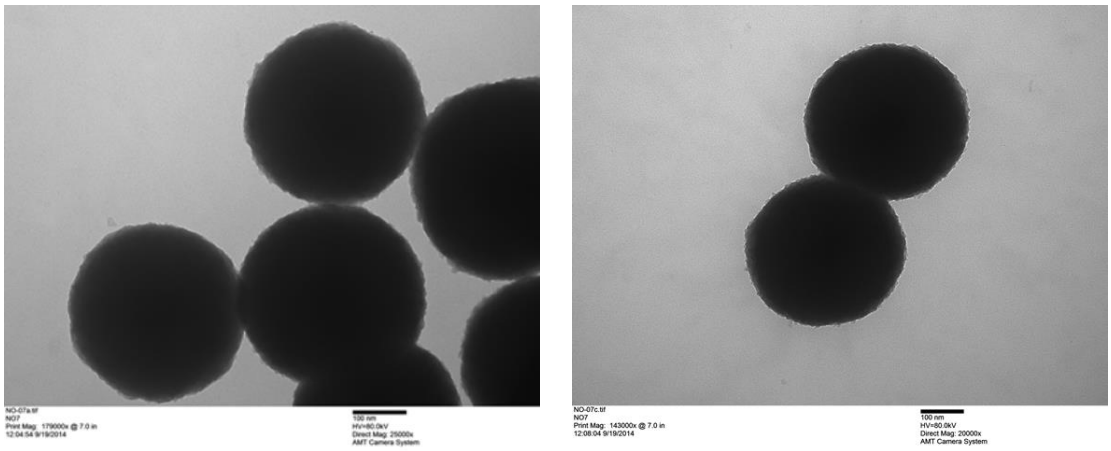

Figure 3.27: TEM images of amine-SSQ particles, Trial 1

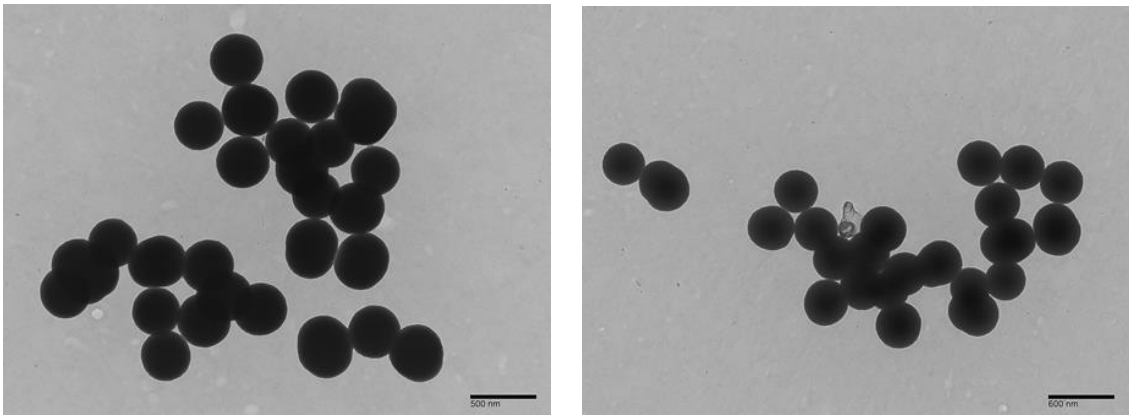

Figure 3.28: TEM images of amine-SSQ particles, Trial 2

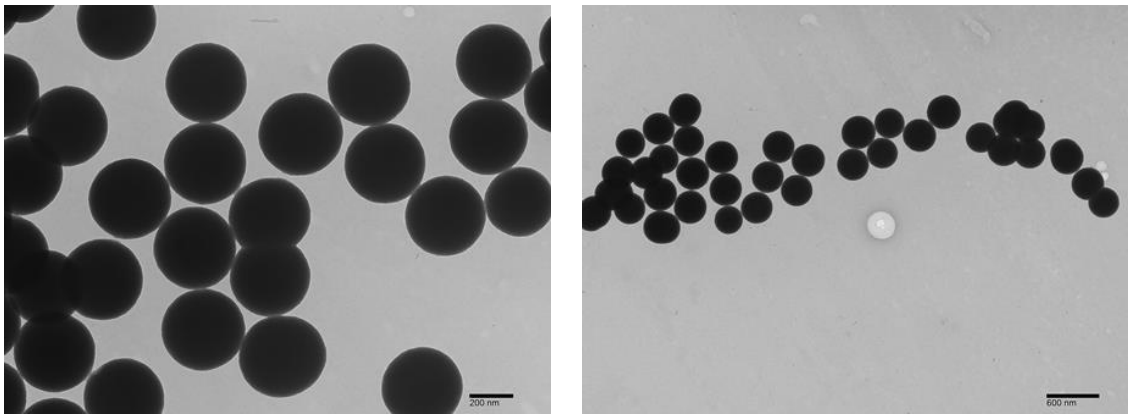

Figure 3.29: TEM images of amine-SSQ particles, Trial 3

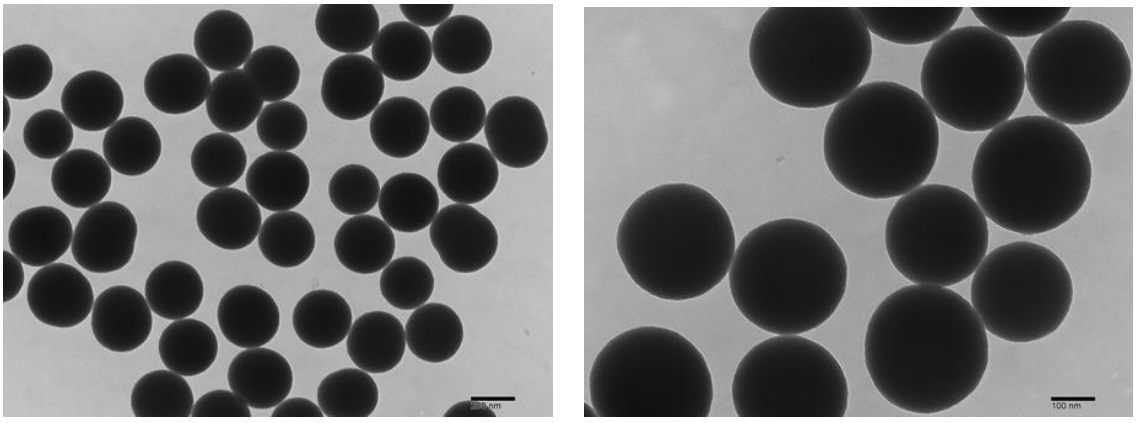

Figure 3.30: TEM images of amine-SSQ particles, Trial 4

3.4.3 Synthesis and characterization of fluorescein functionalized amine-SSQ particles

As depicted in Scheme 3.7, particles were functionalized with fluorescein carboxylic acid via a Steglich esterification in the presence of dicyclohexylcarbodiimide. The reaction was carried out at room temperature for approximately 18 hours to yield a light orange solid. The light orange solid obtained was isolated by repeated centrifugation after re-dispersing the solid in ethanol and water. The silsesquioxane particles obtained in this manner were further characterized by FTIR, UV-visible, fluorescence, and TGA. In the IR spectrum (Figure 3.31), the Si-O-Si stretching frequency at 1044 cm^{-1} confirms the existence of a siloxane network. The stretching frequency at 1641 cm^{-1} represents the carbonyl carbon of fluorescein carboxylic acid which confirms the presence of fluorescein. The stretching frequency at 1548 cm^{-1} represents the N-C stretching frequency, which confirms the successful coupling of fluorescein carboxylic acid to the SSQ's.

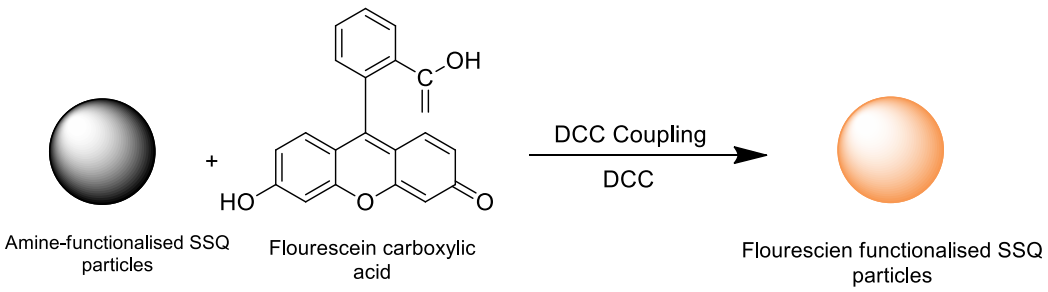

Scheme 3.7: Schematic representation of synthesis of functionalization of amine-SSQ particles with fluorescein carboxylic acid

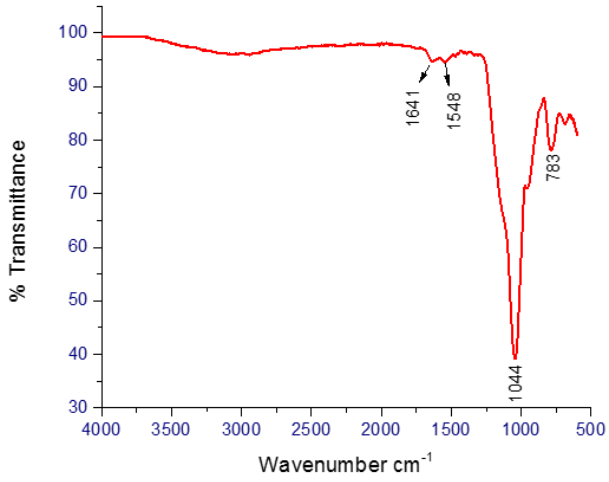

Figure 3.31: FTIR spectrum of fluorescein functionalized amine-SSQ particles

Thermal stability of fluorescein functionalized amine-SSQ particles was also studied using thermogravimetric analysis (Figure A-7). The sample exhibits a three step degradation. In the first degradation step, a weight loss of 2.94% from room temperature to 101 ^{0}C confirms a partial weight loss of alkyl content. From 101 ^{0}C to 530 ^{0}C, the second step degradation was observed with a weight loss of 10.99% refers to the weight loss of alkyl content and fluorescein units. The third step degradation was observed at 530 ^{0}C with a weight loss of 5.83% corresponding to the loss of total organic content. A total weight loss of 19.76% was observed corresponding to the total organic content. The degradation from 668 ^{0}C to 800 ^{0}C corresponds to the degradation of the siloxane network with a weight loss of 1.0%.

3.4.4 Morphology of fluorescein functionalized amine-SSQ particles

The morphology of fluorescein functionalized amine-SSQ particles were studied using TEM. The shape and size of the particles remained the same post functionalization. The TEM images of post functionalized particles confirmed the size and shape of the

particles (Figure 3.32). The successful incorporation of the fluorescence was confirmed using a UV-Vis and fluorescence spectrometer.

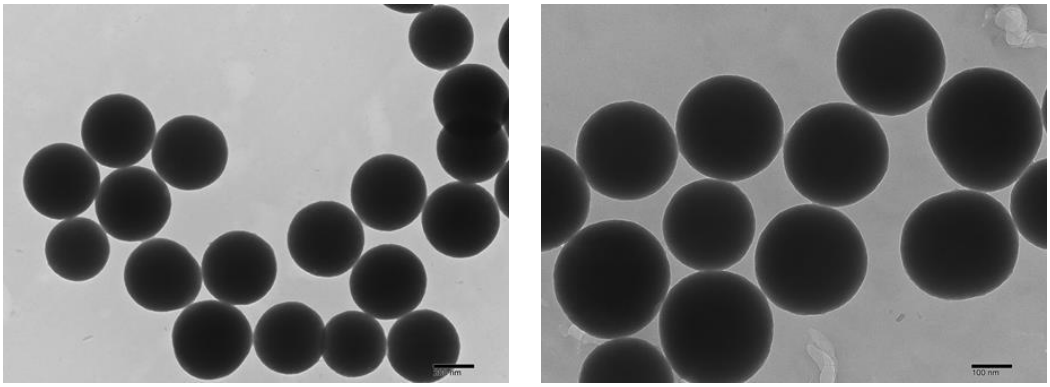

Figure 3.32: TEM images of fluorescein functionalized amine-SSQ particles

3.4.5 Photophysical properties

The photophysical properties of amine-SSQ particles with fluorescein carboxylic acid were studied in ethanol solution. As shown in Figure 3.33(a), a distinct peak at wavelength 514 nm was observed characteristic of fluorescein carboxylic acid which confirms the presence of fluorescein carboxylic acid attached to the amine-SSQ particles. The fluorescence emission spectrum was obtained in ethanol solution and is shown in Figure 3.33(b). The emission spectrum shows a maximum emission at 536 nm upon excitation at 520 nm. The emission spectrum clearly shows s vibronic band at wavelength 536 nm indicating the attachment of fluorescein carboxylic acid moieties.

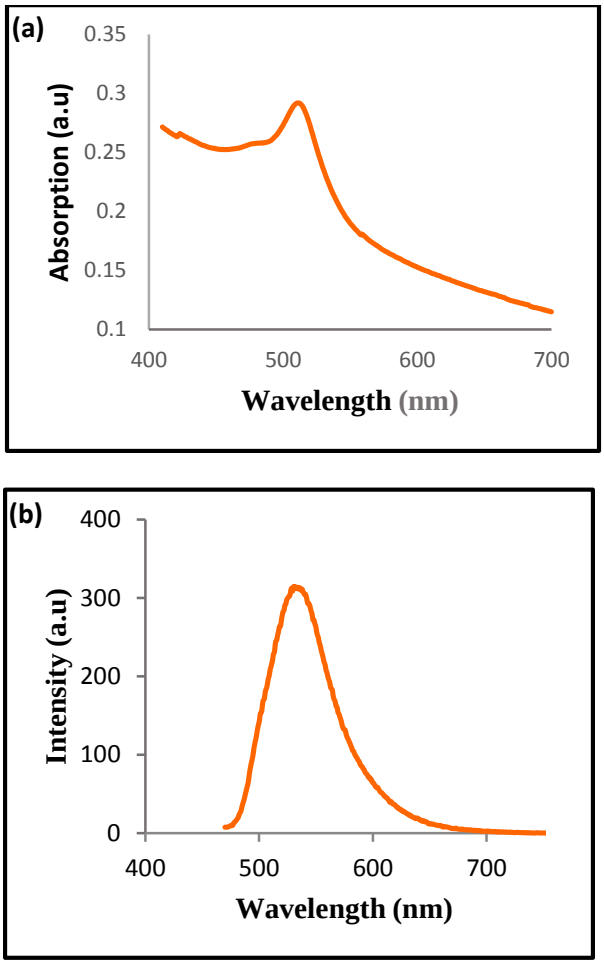

Figure 3.33: (a) UV-Vis absorption spectrum, (b) Fluorescence emission spectrum in ethanol solution (excited at 520 nm)

Successful synthesis of three different silsesquioxane particles with various size ranges was achieved. The control of particles size and morphology was achieved by changing the base concentration and the volume of ethanol. In BC-SSQ, the size and morphology of the particles were dependent on the base concentration, while there was no effect on the size of particles from the change in solvent volume. BC-amine-SSQ particles were dependent on the base concentration but there was no effect on the solvent volume as observed in the preparation of BC-SSQ particles. But with the amine-SSQ

particles, a change in the base concentration as well as volume of the solvent did affect on the size and morphology of the particles. However, the size distribution was very narrow and only limited to microparticles.

3.5 Self-assembly of BC-amine-SSQ particles

In order to self-assembly of SSQ particles, spin coating technique was applied on a polymer coated indium tin oxide (ITO) glass substrate. Polystyrene and polyvinylpyrrolidone polymers were used as the polymer coating. Different concentrations of the particles were prepared to self-assemble on the polymer coated ITO glass. Figure 3.34 is a schematic representation of the process for the self-assembly technique developed in this work.

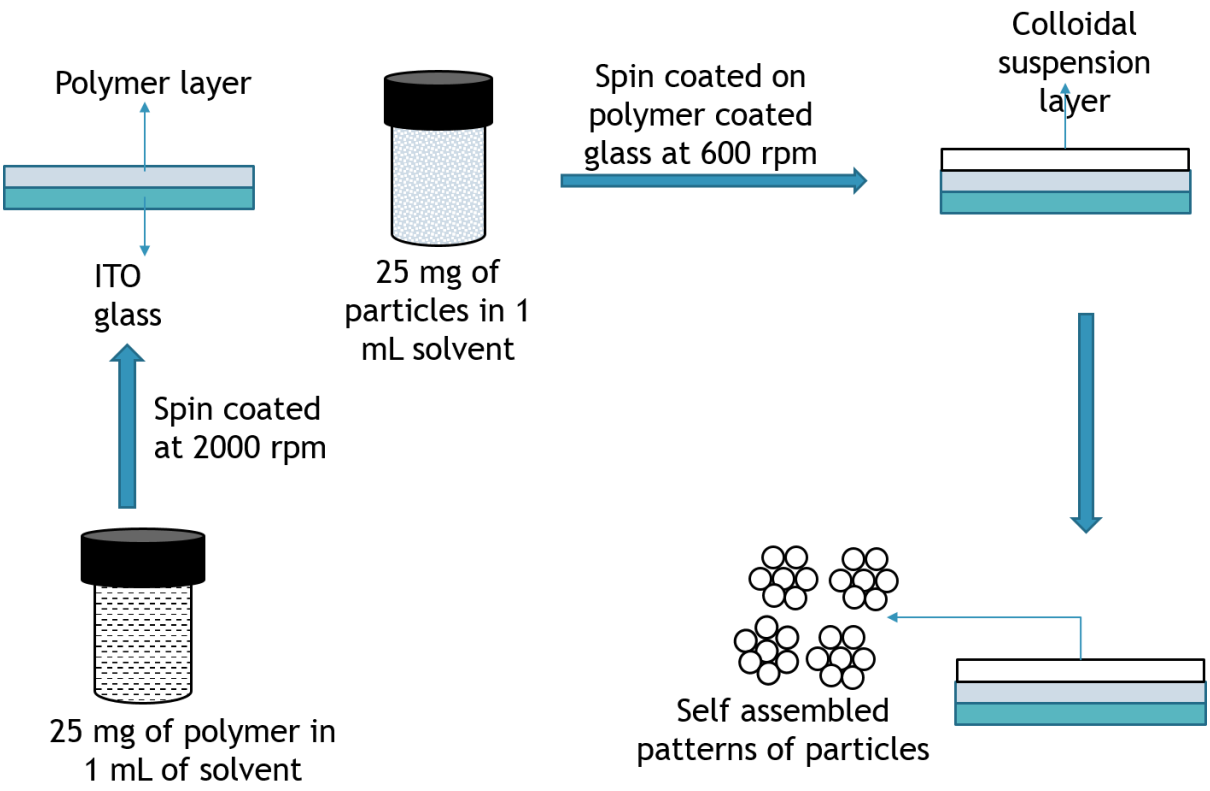

Figure 3.34: Schematic representation of the self-assembly technique

3.5.1 Procedure for the preparation of the polystyrene coated substrate via spin coating

Three different concentrations of SSQ particles were prepared for the self-assembly process. In a 5 mL vial, 25 mg of BC-amine-SSQ particles were dispersed in 1 mL of solvent mixture (a mixture of 0.5 mL ethanol and 0.5 mL distilled water) and labelled as Concentration-1. Similarly, 12.5 mg of BC-amine-SSQ particles were dispersed in 1 mL of the solvent mixture to the sample, Concentration-2, and 6.25 mg of BC-amine-SSQ particles were dispersed in 1 mL to prepare the sample, Concentration-3.

ITO glass plates was cleaned by repeated cleansing with dichloromethane, washed with mild detergent, and rinsed thoroughly with distilled water prior to the blow dry with argon gas. A solution of 25 mg of polystyrene in chlorobenzene was spin coated on cleaned ITO glass plates at 2000 rpm for about 250 seconds. Immediately 300 µL of solution with Concentration-1 was spin coated at 600 rpm for about 250 seconds and the ITO glass substrate was characterized using SEM to visualize the particles assemblies.

3.5.2 Characterization of self-assembly of the particles

The spin-coated ITO glass was examined under SEM in order to study the self-assembly of particles. Solution from Concentration-1 was spin coated on ITO glass plates without the polymer layer and taken as control for the study of self-assembly properties. The control experiments exhibited a monolayer of particles scattered on the base ITO substrate as depicted in Figure 3.35. There were no ordered arrangement of particles observed in this case.

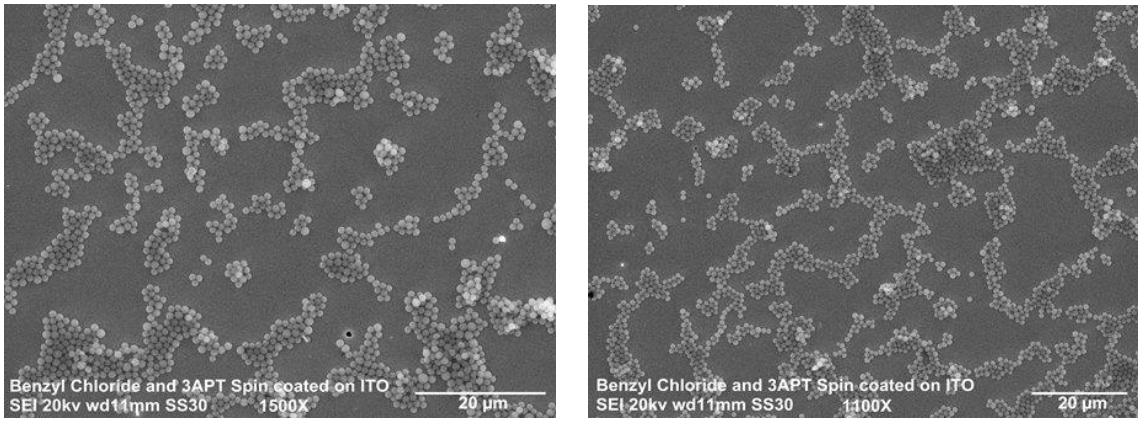

Figure 4.35: SEM images recorded in two different areas of BC-amine-SSQ particles spin coated on ITO glass without a polymer layer (control)

The Concentration-1 solution was spin coated on the polystyrene coated ITO glass substrate at 600 rpm for 250 seconds. Assemblies of randomly scattered colloidasomes were observed (Figure 3.36). These large assemblies of particles appeared to be in a three dimensional arrangement. The assemblies were spherical or oval in shape. However, the consistency of the shape and size of these assemblies in Concentration-1 were random in nature.

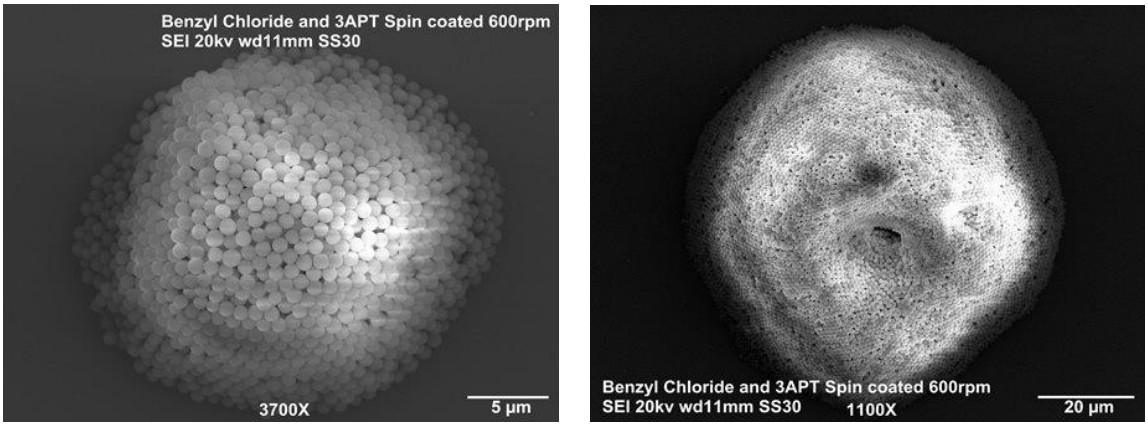

Figure 3.36: SEM images of samples prepared by spin coating Concentration-1 on polystyrene coated ITO glass substrates at 3700X and 1100X

On the other hand, large aggregates with irregular micro-assemblies were observed from the spin coated thin film of the Concentration-2 solution on the polystyrene coated ITO glass substrates (Figure 3.37). The uniformity of assemblies was consistent, but the range of sizes and shapes of the assemblies varied widely and the presence of spherical colloidasomes was rare.

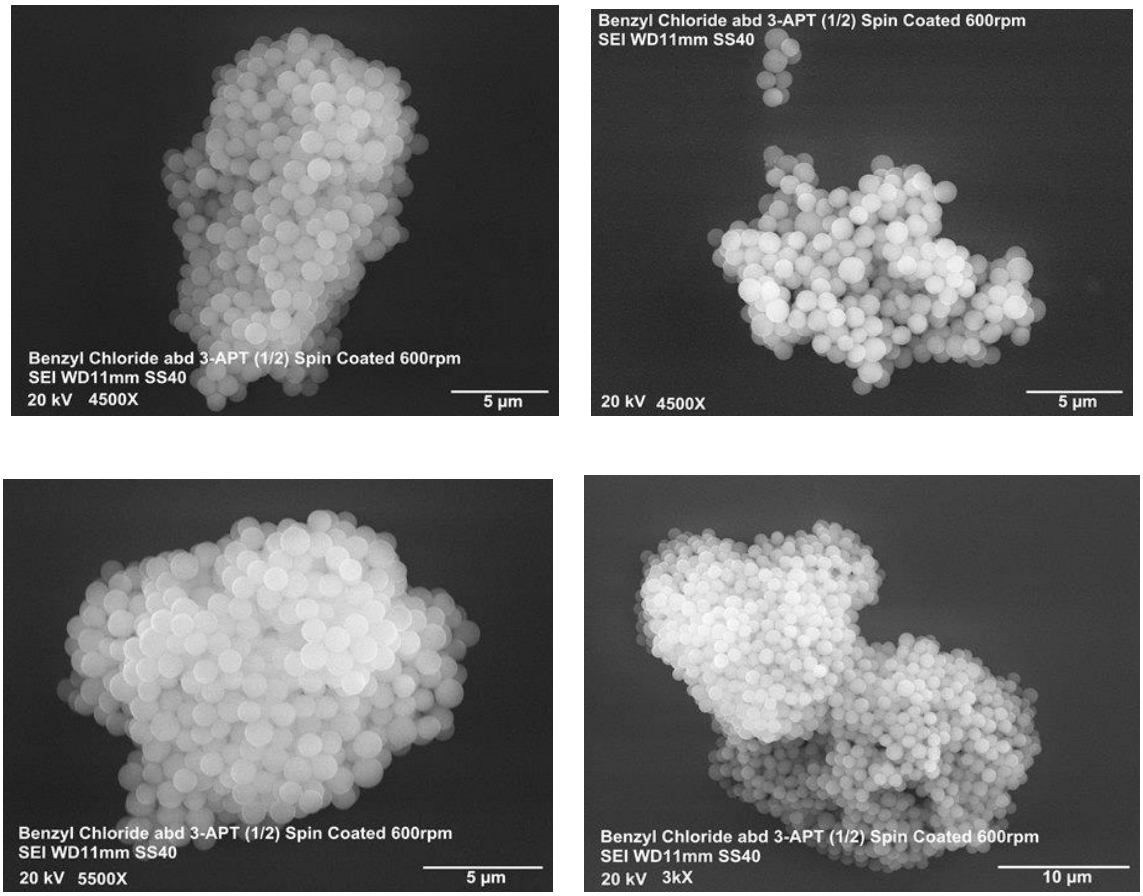

Figure 3.37: SEM images of Concentration-2 solution spin coated on polystyrene coated ITO glass substrates at different magnifications showing disperse nature of assemblies

Uniform self-assemblies of particles were observed when Concentration-3 solution was spin coated on polystyrene coated ITO glass substrates at 600 rpm for 250 seconds (Figure 3.38). The assemblies were approximately spherical in shape with uniform distribution. From these observations, it is clear that consistent patterns of assemblies were obtained from lowest concentration (Concentration-3) of BC-amine-SSQ's.

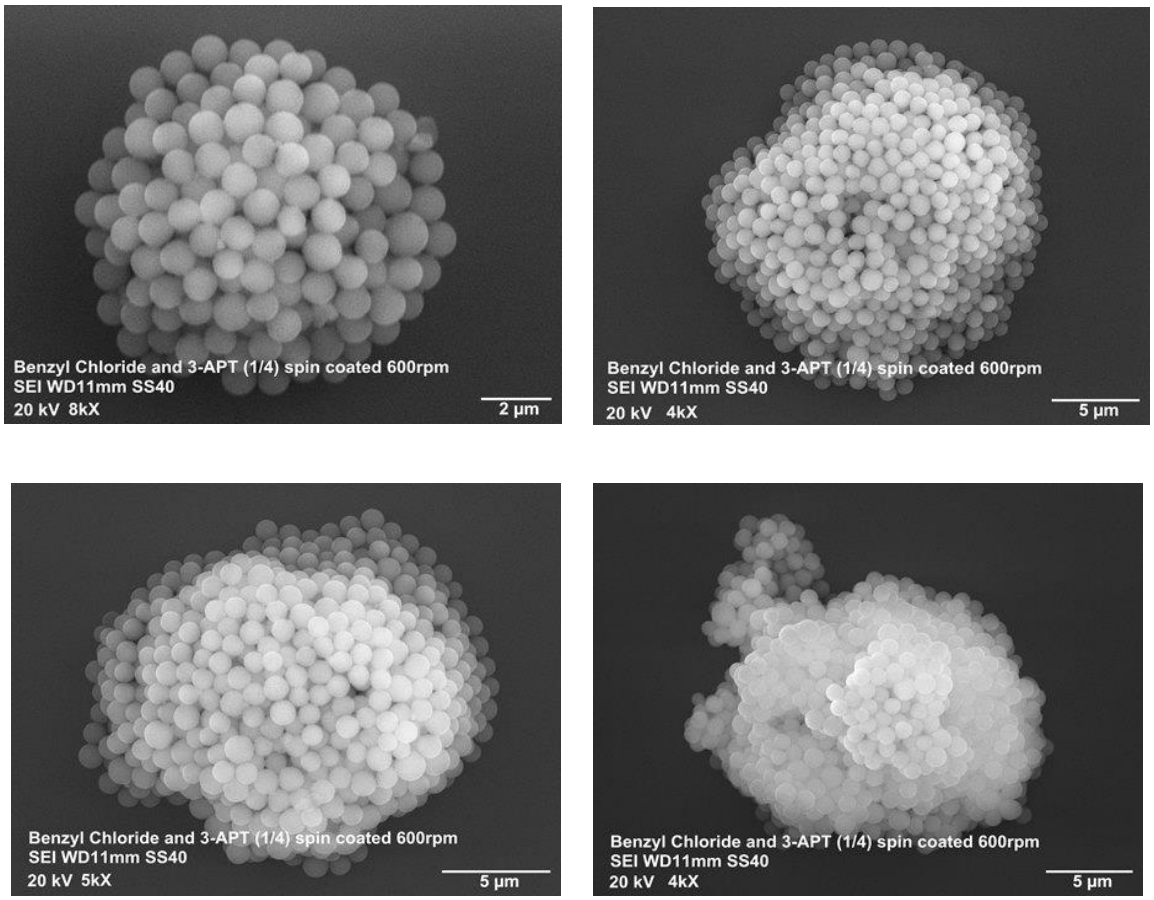

Figure 3.38: SEM images of assemblies obtainedn by spin coating Concentration-3 on polystyrene coated ITO glass substrates at different magnification/regions

3.6. Self-assembly of BC-amine-SSQ particles on polyvinylpyrrolidone (PVP)

3.6.1 Procedure for the preparation of the substrate via spin coating

Solutions with Concentration-1, Concentration-2, and Concentration-3 prepared using the above procedures described in section 3.5.1 were used for the study of their assembling properties on PVP coated ITO glass substrates.

PVP solution prepared by dissolving 25 mg in 1 mL of chlorobenzene was spin coated on cleaned ITO glass plates at 2000 rpm for about 250 seconds to obtain the PVP coated ITO substrates. A solution of BC-amine-SSQ particles of Concentration-1, Concentration-2, and Concentration-3 were spin coated at 600 rpm for about 250 seconds and the resulting samples were imaged by SEM for the assembly of particles on PVP coated substrates.

4.6.2 Characterization of self-assembly of particles

The SEM images of the assemblies of particles from Concentration-1 are presented in Figure 3.39. The above sample showed a monolayer of small self-assemblies. However, the self-assemblies were inconsistent, with irregular shapes and an uneven distribution throughout the substrate. Most areas of the substrate were covered with monolayers of particles.

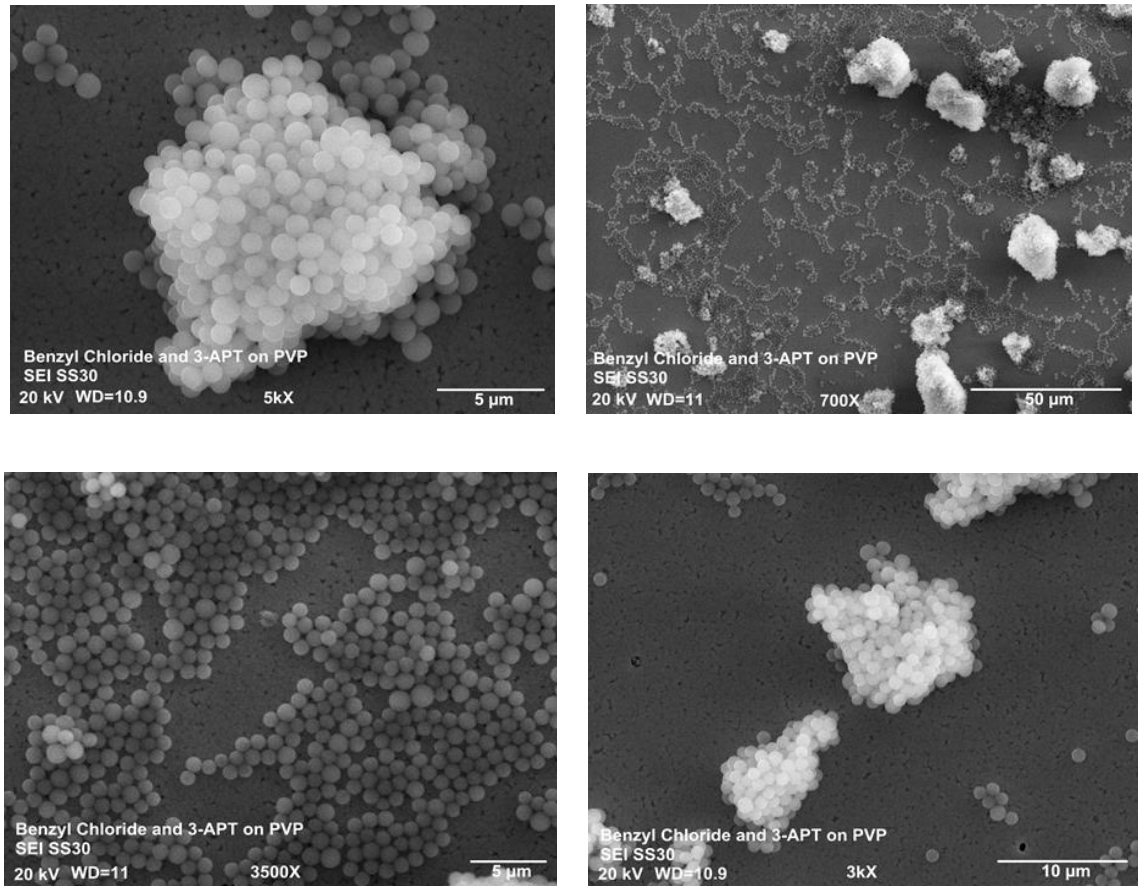

Figure 3.39: SEM images of assemblies obtainedn by spin coating Concentration-1 on PVP coated ITO glass substrates at different magnification/regions

The assembly of particles of Concentration-2 on PVP coated ITO glass is shown in Figure 3.40. Concentration-2 particles were spin coated on PVP coated ITO glass at 600 rpm for 250 seconds. There was a one-dimensional layer of particle self-assemblies observed within the polymer layer. It is a very distinct layer of particles coated with a polymer layer. This may be due to the polymer coating dissolving in the particle solution, since PVP is highly soluble in water.

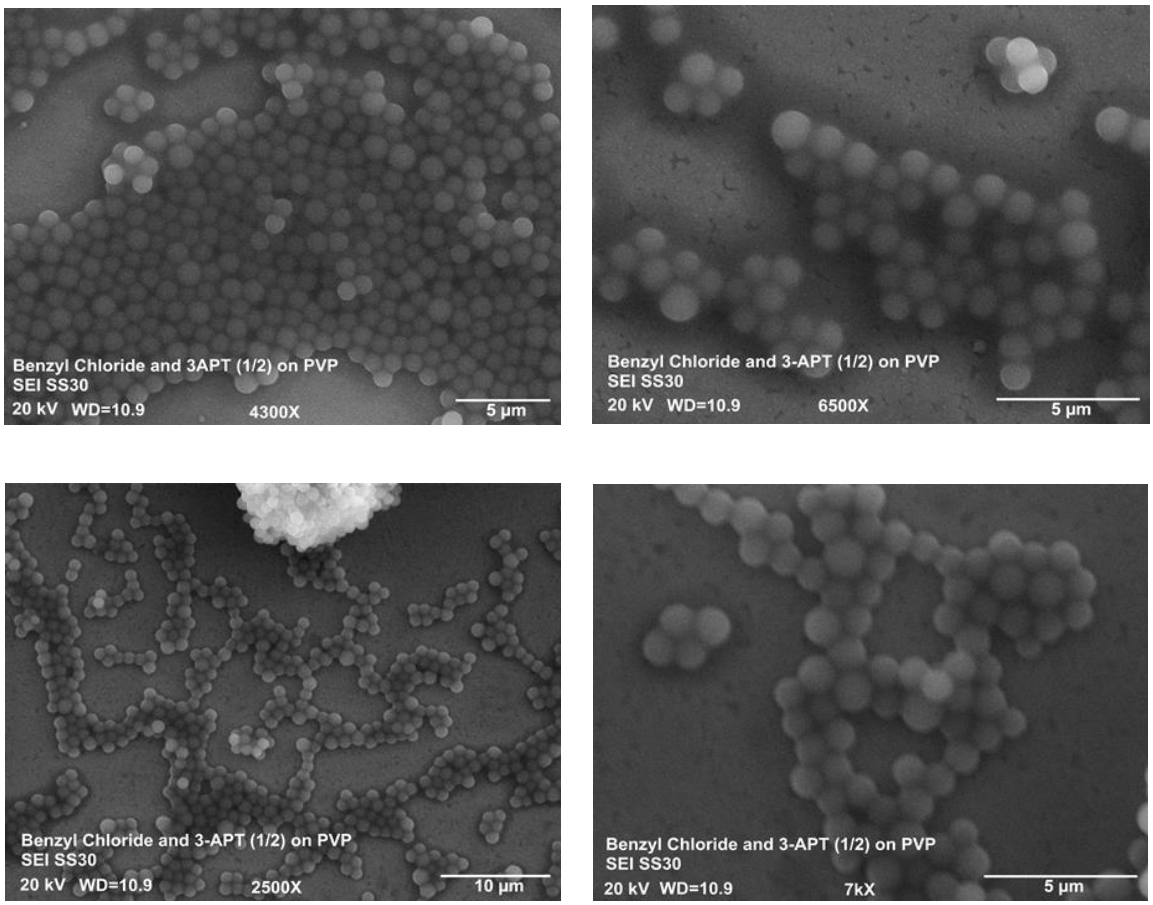

Figure 3.40: SEM images of assemblies obtained by spin coating Concentration-2 on PVP coated ITO glass substrates at different magnification/regions

The assembly of the particles of Concentration-3 on PVP coated ITO glass is shown in the Figure 3.41. When the Concentration-3 solution was spin coated on PVP coated ITO glass substrates at 600 rpm for 250 seconds, the particles were found to be mostly scattered showing no particular arrangement.

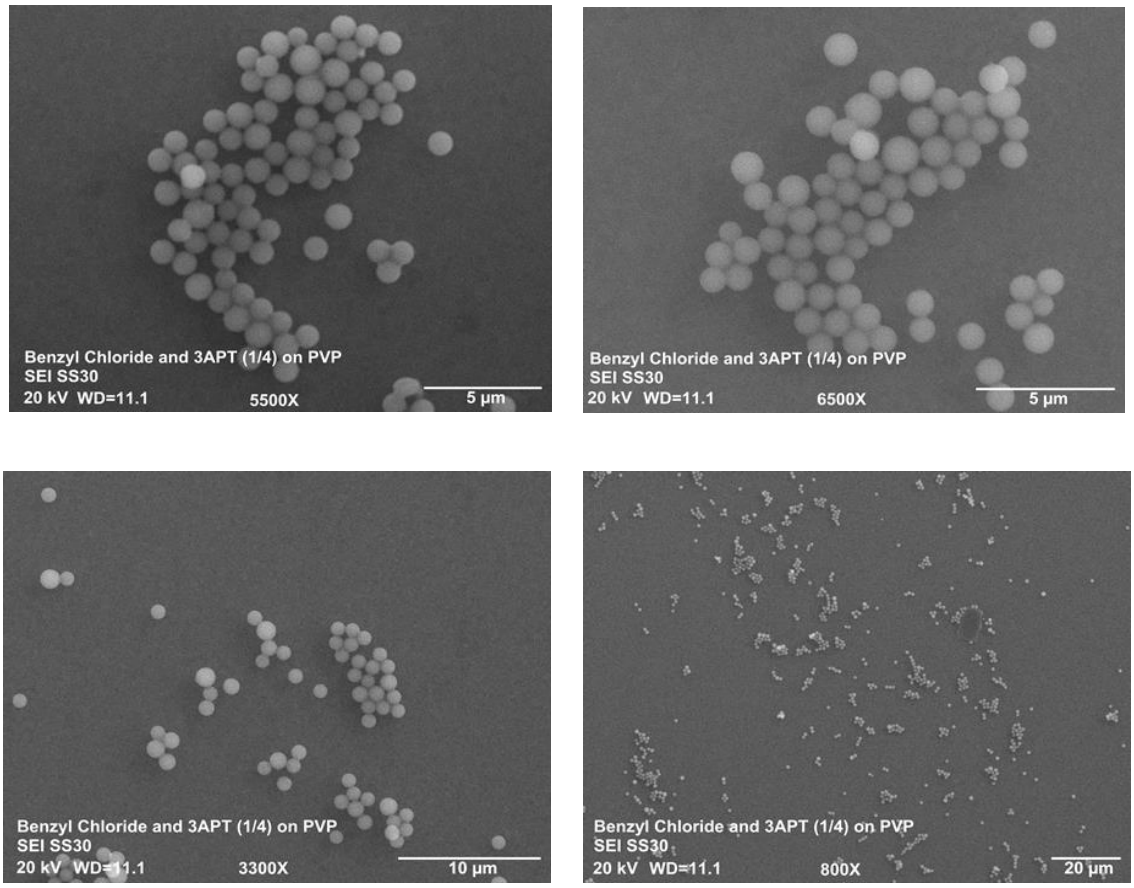

Figure 3.41: SEM images of assemblies obtained by spin coating Concentration-3 on PVP coated ITO glass substrates at different magnification/regions.

A successful technique was developed via spin coating for the self-assembly of the functionalized SSQ particles. It was observed that the formation of self-assemblies were dependent on the type of polymer and the concentration of the colloidal suspension. From the above results, it is clear that the PVP polymer coated ITO glass, spin coated with Concentration-3 yielded consistent self-assemblies with uniform distribution. Also, these results further evidence that particles interaction with polystyrene polymer is higher compared to that of with PVP substrate due to the hydrophilic and hydrophobic nature of polystyrene and PVP.

CHAPTER 4

MATERIALS AND EXPERIMENTAL METHODS

4.1 Materials

p-(chloromethyl)phenyl trimethoxy silane (benzyl chloride trimethoxy silane) was purchased from Gelest Inc. Tetraethoxysilane (TEOS) and 3-aminopropyltriethoxysilane (3-APT silane) was purchased from Alfa Aesar. Anhydrous ethanol (200 proof), ammonium hydroxide (28%), dichloromethane, rhodamine-B carboxylic acid, 9-anthracene methanol, N,N'-Dicyclohexylcarbodiimide (DCC) and fluorescein sodium salt were obtained from Sigma Aldrich. All the chemicals are used as received without any purification unless mentioned.

4.2 Characterization

Transmission Electron Microscopy (TEM) characterizations were performed on a JEOL 1400plus with AMT XR81 digital camera at 80 KeV. Scanning Electron Microscopy (SEM) characterizations were performed on JEOL JSM-6510LV. FT-IR spectra were obtained using a Perkin Elmer Spectrum One FTIR with universal ATR sampling accessory. Thermogravimetric analysis was performed with a 2950 TGA HR at the WKU Thermal Analysis Lab. The elemental analysis was performed using CHN analyzer at the Advanced Material Institute, Western Kentucky University. The photophysical properties were performed on a fluorescence spectrometer, Perkin Elmer LS 55 and a UV-Visible spectrometer, Perkin Elmer, Lambda 35.

4.3 Experimental procedures for the synthesis of functionalized particles

4.3.1. Synthesis of benzyl chloride silsesquioxane (BC-SSQ) particles

To a 20 mL scintillator vial, anhydrous ethanol (10 mL) and 28% ammonium hydroxide (1 mL, 7.20 mmol) was added and was allowed to stir for 5 minutes. Benzyl chloride trimethoxy silane (1.8 mL, 8.16 mmol) was added dropwise to the above mixture at a rate of 0.5 mL for every 2 minutes and was allowed to stir overnight (approximately 18 hours) at room temperature. The white solid obtained was separated from the solution by centrifugation for 20 minutes at 3000 rpm. The supernatant was discarded and the precipitate was re-dispersed in ethanol to remove excess ammonium hydroxide and unreacted benzyl chloride silane and was centrifuged for 20 minutes at 3000 rpm. The supernatant was discarded and the precipitate was re-dispersed in distilled water to remove any water soluble impurities and continued with repeated centrifugation for 20 minutes at 3000 rpm. The white solid obtained was dried under vacuum for 24 hours (Yield by weight, 94.59 %). FT-IR (cm^{-1}): 3089 (Alkyl C-H), 1605 (aromatic C=C from benzyl chloride), 1396, 1275, (Si-C), 1125-1039 (Si-O-Si), 831-642 (aromatic); Elemental analysis: Theoretical – C 43.1%, H 3.6% ($C_7H_7ClSiO_{2.5}$); Experimental – C 43.8%, H 3.1%.

4.3.2 Functionalization of BC-SSQ particles with anthracene methanol

In a 100 mL one-neck round bottom flask, 500 mg of BC-SSQ particles were dispersed in 30 mL of anhydrous ethanol and was allowed to stir for 5 minutes until all the solid was dispersed completely in ethanol. Potassium carbonate was used as a catalyst. Potassium carbonate (79 mg, 0.57 mmol, which was 1.2 equivalents to 9-

anthracene methanol) was added to the flask along with 9-anthracene methanol (100 mg, 0.48 mmol) was added and allowed to stir overnight (approximately 18 hours) at room temperature. The flask was covered with aluminium foil to keep the reaction away from visible light. The pale yellow solid was separated from the solution by centrifugation for 20 minutes at 3000 rpm. The supernatant was discarded and the precipitate was re-dispersed in ethanol to remove excess of potassium carbonate and was centrifuged for 20 minutes at 3000 rpm. The supernatant was discarded and the precipitate was re-dispersed in distilled water to remove any water soluble impurities and continued with repeated centrifugation for 20 minutes at 3000 rpm. The pale yellow solid obtained was dried under vacuum for 24 hours to yield 354 mg (70.8%, by weight) fluorescent tag functionalized particles. FT-IR (cm^{-1}): 3022-2990 (Alkyl C-H), 1605 (aromatic C=C from benzyl chloride), 1396, 1263, and 1213 (Si-C), 1124-1019 (Si-O-Si), 832-672 (aromatic). UV-visible in solution - λ_{max} (nm) – 330, 347, 365, and 384; PL emission λ_{max} (nm) – 392, 414, and 439.

4.3.3 Synthesis of binary reactive groups functionalized benzyl chloride-amine (BC-Amine-SSQ) particles

In a 100 mL one-neck round bottom flask, anhydrous ethanol (65 mL) and 28% ammonium hydroxide (3.5 mL, 25 mmol) were allowed to stir for 5 minutes. 3-APT silane (2 mL, 8.50 mmol) was added to the flask dropwise and immediately benzyl chloride trimethoxy silane (1 mL, 4.53 mmol) was added dropwise to the flask and was allowed to stir overnight (approximately 18 hours) at room temperature. The white solid obtained was separated from the solution by centrifugation for 20 minutes at 3000 rpm. The supernatant was discarded and the precipitate was re-dispersed in ethanol to remove

excess of ammonium hydroxide and were centrifuged for 20 minutes at 3000 rpm. The supernatant was discarded and the precipitate was re-dispersed in distilled water to remove any water soluble impurities and continued with repeated centrifugation for 20 minutes at 3000 rpm. The white solid obtained was dried under vacuum for 24 hours (yield by weight, 43.18%). FT-IR (cm^{-1}): 2997 (Alkyl C-H), 1605 (aromatic C=C from benzyl chloride), 1397, 1264 (Si-C), 1127-1020 (Si-O-Si), 844-694 (aromatic); Elemental analysis: Theoretical – C 39.4%, H 4.9%, N 4.5%; Experimental – C 39.4 %, H 3.8%, N 0.8%.

4.3.4 Functionalization of BC-amine SSQ particles with 9-anthracene methanol and rhodamine-B - Selective functionalization with two fluorescent tags

In a 100 mL one-neck round bottom flask, BC-Amine SSQ particles (1.0 g) were dispersed in anhydrous ethanol (60 mL) and the mixture was allowed to stir until all the solid was dispersed completely in ethanol. Potassium carbonate (199 mg, 1.15 mmol which was 1.2 equivalents to 9-anthracene methanol) was added to the flask and then 9-anthracene methanol (250 mg, 1.2 mmol) was added and was allowed to stir overnight (approximately 18 hours) at room temperature. The flask was covered with aluminium foil to keep the reaction away from visible light. The pale yellow solid was separated from the solution by repeated centrifugation for 20 minutes at 3000 rpm. The supernatant was discarded and the precipitate was re-dispersed in ethanol to remove excess of anthracene and potassium carbonate and were centrifuged for 20 minutes at 3000 rpm. The supernatant was discarded and the precipitate was re-dispersed in distilled water to remove any water soluble impurities and continued with repeated centrifugation for 20

minutes at 3000 rpm. The pale yellow solid obtained was dried under vacuum for 24 hours to yield 928 mg, (92% by weight) fluorescent tag functionalized particles.

These above dried anthracene functionalized particles (928 mg) were taken in a 250 mL one neck round bottom flask and were dispersed in dichloromethane (100 mL). N,N'-dicyclohexylcarbodiimide (DCC) (170 mg, 0.82 mmol, which was 1.2 equivalents to rhodamine B) was added to the flask and then rhodamine-B (330 mg, 0.68 mmol) was added to the flask followed by purging with argon gas for 45 minutes. The reaction mixture was allowed to stir overnight (approximately 18 hours) at room temperature. The pink solid obtained was separated by repeated centrifugation for 20 minutes at 3000 rpm. The supernatant was discarded and the precipitate was re-dispersed in ethanol to remove excess DCC and was centrifuged for 20 minutes at 3000 rpm. The supernatant was discarded and the precipitate was re-dispersed in ethanol and continued with repeated centrifugation for 20 minutes at 3000 rpm. The pink solid obtained was dried under vacuum for 24 hours to yield 856 mg (92%, by weight). FT-IR (cm^{-1}): 2981 (Alkyl C-H), 1606 (aromatic C=C from benzyl chloride), 1442 (N-C), 1396-1261 (Si-C), 1123-1019 (Si-O-Si), 832-642 (aromatic).

UV-visible in solution - λ_{max} (nm) – 273 and 356 (presence of anthracene); PL emission λ_{max} (nm) – 398, 419, and 445 (presence of anthracene) and 590 (presence of rhodamine B).

4.3.5 Functionalization of BC-amine SSQ particles with rhodamine-B

In a 100 mL one-necked round bottom flask, BC-amine SSQ particles (1.0 g) were dispersed in dichloromethane (100 mL). DCC (170 mg, 0.82 mmol which was 1.2 equivalents to rhodamine-B) was added to the flask along with rhodamine-B (330 mg, 0.68 mmol). The mixture was purged under argon gas for 45 minutes, and followed by allow to stir overnight (approximately 18 hours) at room temperature. The pink solid was separated from the solution by repeated centrifugation for 20 minutes at 3000 rpm. The supernatant was discarded and the precipitate was re-dispersed in ethanol to remove excess DCC and then centrifuged for 20 minutes at 3000 rpm. The supernatant was discarded and the precipitate was re-dispersed in ethanol and continued with repeated centrifugation for 20 minutes at 3000 rpm. The pink solid obtained was dried under vacuum for 24 hours to yield 937 mg (93%, by weight). FT-IR (cm^{-1}): 2988 (Alkyl C-H), 1605 (aromatic C=C from benzyl chloride), 1442 (N-C), 1396-1261 (Si-C), 1124-1020 (Si-O-Si), 832-690 (aromatic).

UV-visible in solution - λ_{max} (nm) – 555; PL emission λ_{max} (nm) – 560.

4.3.6. Synthesis of amine functionalized SSQ particles (Amine-SSQ)

In a 100 mL one-necked round bottom flask, anhydrous ethanol (20 mL) and 28% ammonium hydroxide (6 mL, 43 mmol) was added and allowed to stir for 5 minutes. Tetraethoxysilane (1 mL, 4.5 mmol) was added to the flask dropwise and immediately 3-APT silane (3 mL, 12.8 mmol) was added dropwise and then allowed to stir overnight (approximately 18 hours) at room temperature. The white solid obtained was separated from the solution by repeated centrifugation for 20 minutes at 3000 rpm. The supernatant

was discarded and the precipitate was re-dispersed in ethanol to remove excess of ammonium hydroxide and was centrifuged for 20 minutes at 3000 rpm. The supernatant was discarded and the precipitate was re-dispersed in distilled water to remove any water soluble impurities and continued with repeated centrifugation for 20 minutes at 3000 rpm. The white solid obtained was dried under vacuum for 24 hours (Yield by weight, 19.2%). FT-IR (cm^{-1}): 1044 (Si-O-Si).

4.3.7. Preparation of fluorescein carboxylic acid from fluorescein sodium salt

In a 100 mL beaker, fluorescein sodium salt (1 g, 0.26 mmol) was completely dissolved in distilled water (50 mL). To this solution, 3.0 M hydrochloric acid was added dropwise until the solution turns acidic while monitoring the acidity of the solution using a pH paper. (pH paper changing its colour to purple, pH = 2.5). The resulted dark orange solid was separated from the solution by vacuum-filtration and the solid was dried under vacuum for 24 hours at 50^{o} C.

4.3.8. Functionalization of amine functionalized SSQ particles with fluorescein carboxylic acid

In a 100 mL one-necked round bottom flask, 100 mg of amine functionalized SSQ particles were dispersed in dichloromethane (20 mL). DCC (70 mg, 0.34 mmol, which was 1.2 equivalent to fluorescein carboxylic acid) was added to the flask and then fluorescein carboxylic acid (100 mg, 0.28 mmol) was added and purged under argon gas for 45 minutes, and then allowed to stir overnight (approximately 18 hours) at room temperature. The light orange solid obtained was separated by repeated centrifugation for 20 minutes at 3000 rpm. The supernatant was discarded and the precipitate was re-

dispersed in ethanol to remove excess of DCC and were centrifuged for 20 minutes at 3000 rpm. The supernatant was discarded and the precipitate was re-dispersed in ethanol and continued centrifugation for 20 minutes at 3000 rpm. The light orange solid obtained was dried under vacuum for 24 hours to yield 89 mg (89%, by weight). FT-IR (cm^{-1}): 1641 (C=O from carbonyl carbon of fluorescein carboxylic acid), 1548 (N-C), 1044 (Si-O-Si).

UV-visible in solution - λ_{max} (nm) – 514; PL emission λ_{max} (nm) – 536.

CHAPTER 5

CONCLUSION

The goal of this project was to synthesize benzyl chloride functionalized silsesquioxane particles and to develop a novel technique to produce ordered self-assemblies. Benzyl chloride silsesquioxane particles were successfully synthesized by the Stöber method using benzyl chloride trimethoxy silane as the precursor. Successful control of size and morphology of particles was achieved by optimizing the molar amount of base and the silane, and the volume of ethanol. These particles were successfully functionalized with anthracene blue fluorescent tag and their photophysical properties were studied in ethanol solution. The UV-Vis spectrum confirms the successful incorporation of anthracene moieties to the silsesquioxane network. The binary reactive groups of benzyl chloride and amine functionalized silsesquioxane particles were also successfully synthesized via hydrolysis and co-condensation reaction using benzyl chloride trimethoxy silane and 3-APT silane as precursors. The control of particle size and their morphologies was successfully achieved by optimizing experimental parameters. These particles were successfully multi-functionalized with anthracene and rhodamine-B. The photophysical properties of functionalized BC-amine-SSQ particles were studied, confirming the incorporation of rhodamine dye. BC-amine SSQ particles were also successfully functionalized with rhodamine-B. The UV-Vis spectrum of rhodamine grafted particles exhibit a single peak at 560 nm and the fluorescence spectrum exhibits maximum fluorescence emission at 580 nm, which confirms the presence of rhodamine-B. The amine-functionalized silsesquioxane particles were successfully synthesized by the Stöber method using tetraethoxy silane and 3-APT

silane precursors. The size and morphology was successfully tuned by varying the base concentration and solvent volume. These particles were successfully functionalized with fluorescein carboxylic acid which confirmed by UV-Vis spectroscopy. An absorption peak at 514 nm and a single sharp peak of emission at 536 nm confirm the presence of the fluorescein carboxylate group.

The spin-coating technique was successfully developed for self-assembling the functionalized silsesquioxane particles. These self-assemblies were observed on polymer coated ITO glass substrates, with a strong dependence on the nature of the polymer layer (polystyrene or PVP) and the concentration of the colloidal suspension. When polystyrene coated ITO glass was used as a substrate, consistent self-assemblies were obtained with the 6.25 mg/mL concentration (Concentration-3) of the colloidal suspension. When PVP coated ITO glass was used as a substrate, monolayers of colloids were observed in all the colloidal suspensions under identical conditions. With PVP coated ITO glass substrate, the particles interaction with the polymer layer and self-assemblies were not observed. By this, we can conclude that polystyrene coated ITO glass substrates are a better choice to form colloidal self-assemblies. Further, the self-assemblies can be fine-tuned by changing the nature of the polymer layer and concentration of the colloidal suspension.

REFERENCES

1. Mori H., *Inter. J. Poly. Sci.,* **2012**.
2. Arkhireeva. A.; Hay J. H., *J. Mater. Chem.*, **2003**, 13, 3122-3127.
3. Douglas A.; Kenneth J. S., *Chem Rev.*, **1995**, 95, 1431-1442.
4. Yu G.; Gao J.; Hummelen J. C.; Wudl F.; Heeger A. J., *Science.*, **1995,** 270, 1789-1791.
5. Karg M.; König T.; Retsch M.; Stelling R.; Reichstein P. M.; Honold T.; Thelakkat M.; Fery A., *Materials Today*, **2015**, 18, 185-205.
6. Zhang J.; Li Z.; Zhang X.; Yang B., *Adv. Mater*., **2010**, 22, 4249-4269.
7. Toolan D. T. W.; Fujji S.; Ebbens S. J.; Nakamura Y.; Howse R. J., *The Royal Chem Soc*., **2014**.
8. Pescarmona P. P.; Maschmeyer T., *Aust. J. Chem*., **2001**, 54, 583-596.
9. Blaaderen A. V.; Vrij A. J., *Colloid Interface Sci.*, **1993**, 156, 1.
10. Suratwala T. I.; Hanna M. L.; Miller E. L.; Whitman P. K.; Thomas I. M.; Ehrmann P. R.; Maxwell R. S.; Burnham A. K., *J. Non-Cryst. Solids*, **2003**, 316, 349'
11. Hatakeyama F.; Kanzaki S., *J. Am. Ceram. Soc.,* **1990**, 73, 2107.
12. Yacoub-George E.; Bratz E.; Tiltscher H., *J. Non-Cryst. Solids*, **1994**, 167, 9.
13. Silva C. R.; Airoldi C., *J. Colloid Interface Sci.*, **1997**, 195, 381.
14. Reynolds K. J.; Colon L. A., *J. Liq. Chromatogr. Relat. Techno.,* **2000**, 23, 161.
15. Etienne M.; Lebeau B.; Walcarius A., *New J. Chem.,* **2002**, 26, 384.
16. Yin R.; Ottenbrite R. M.; Polym. Prepr. **1996**, 36, 265.

17. Arkhireeva. A.; Hay J. H., *Polym. Polym.,* Comp., **2004**, 12, 101.

18. Arkhireeva. A.; Hay J. H.; Manzano M.; Maters H.; Oware W.; Shaw S. J., *J. Sol-gel Sci. Tech.,* **2004**, 31, 31.

19. Arkhireeva. A.; Hay J. H., *J. Mater. Chem.,* **2005**, 17, 875.

20. Organic Solar Cells: Materials, Devices, Interfaces and Modeling. Edited by Qiquan qiao.

21. Yamamoto C.; Okamoto Y., *Bull. Chem. Soc. Jp*m., **2004**, 77, 227-257.

22. Tanaka K.; Ishihuro F.; Chujo Y., *J. Am. Chem Soc*., **2010,** 132, 17649-17651.

23. Zhang F.; Tu Z.; Yu J.; Li H.; Huang C.; Zhang H., *RSC Adv.,* **2013**, 3, 5438-5446.

24. Bronstein L. M.; Linton C. N.; Karlinsey R., *Langmuir*, **2003**, 19, 7071-7083.

25. Acharya S.; Hill J. P.; Ariga K., *Adv. Mater.,* **2009**, 21, 2959.

26. McGorty R.; Fung G.; Kaz D.; Manoharan V. N., *Materials Today*., **2010**, 13, 6, 34-42.

27. Kralchevsky P. A.; Denkov N. D., *Curr. Opin. Colloid Interface Sci.*, **2001**, 6, 383.

28. Micheletto R.; Fukuda H.; Ohtsu M., *Langmuir*, **1995**, 11, 3333.

29. Hayward R. C.; Saville D. A.; Aksay I.A., *Nature*, **2000**, 404, 56.

30. Trau M.; Saville D. A.; Aksay I. A., *Science.,* **1996**, 272, 706.

31. Lumsdon S. O.; Kaler E. W.; Velev O. D., *Langmuir.,* **2004**, 20, 2108.

32. Jiang P.; McFarland J. J., *Am. Chem. Soc.,* **2004**, 126, 13778-13786.

33. Mihi A.; Ocana M.; Miguez H., *Adv. Mater.,* **2006**, 18, 2244-2249.

34. Chen J., *Appl. Surf. Sci.,* **2013**, 270, 6-15.

35. Bartlett A. P.; Pichumani M.; Giuliani M.; González-Vinas W.; Yethiraj A., *Langmuir*, **2012**, 28, 3067-3070.

36. Colson R.; Cloots R.; Henrist C., *Langmuir*, **2011**, 27, 12800-12806.

APPENDIX

TGA Graphs

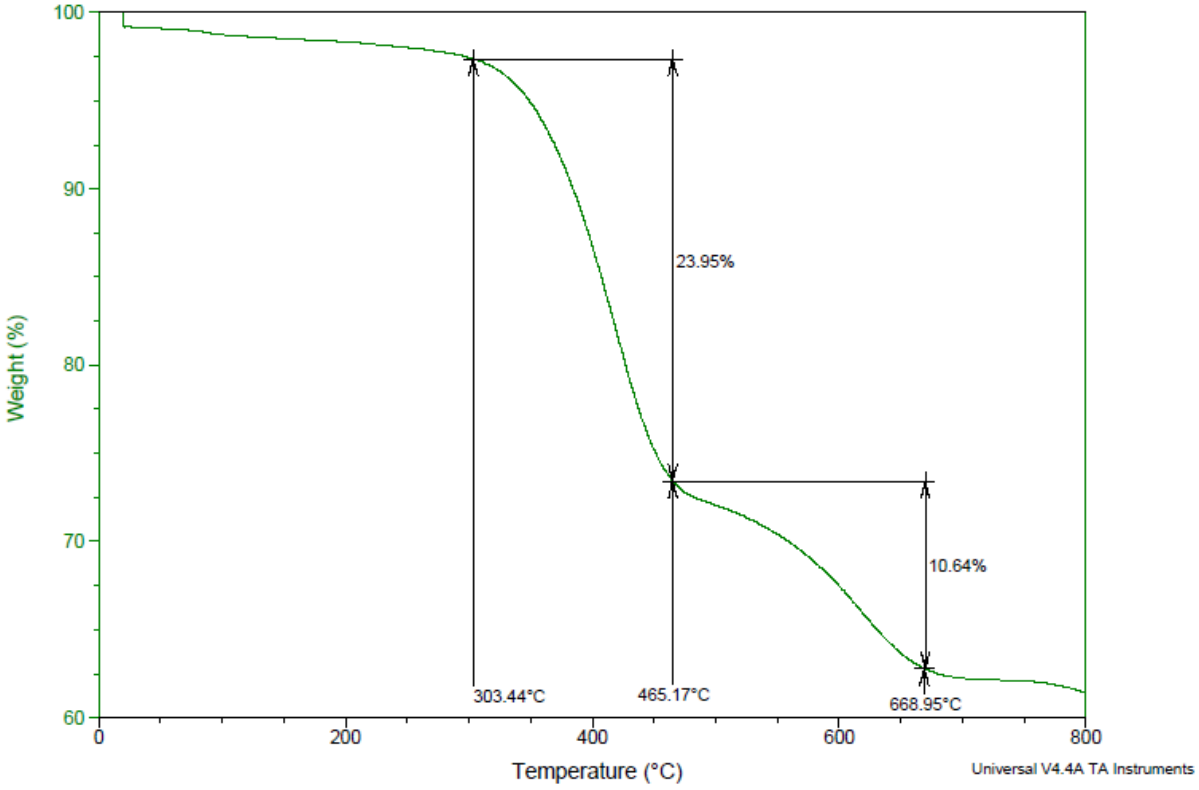

Figure A-1: TGA plot of BC-SSQ particles

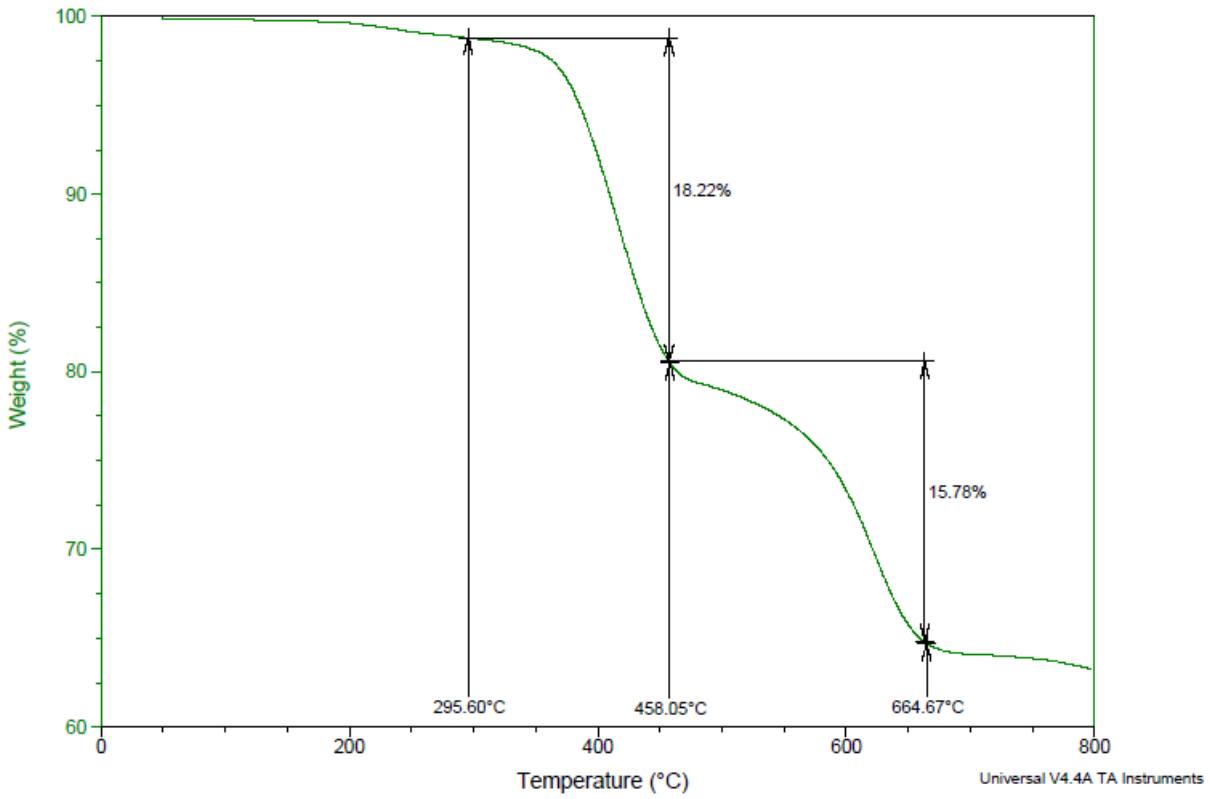

Figure A-2: TGA plot of anthracene functionalized BC-SSQ particles

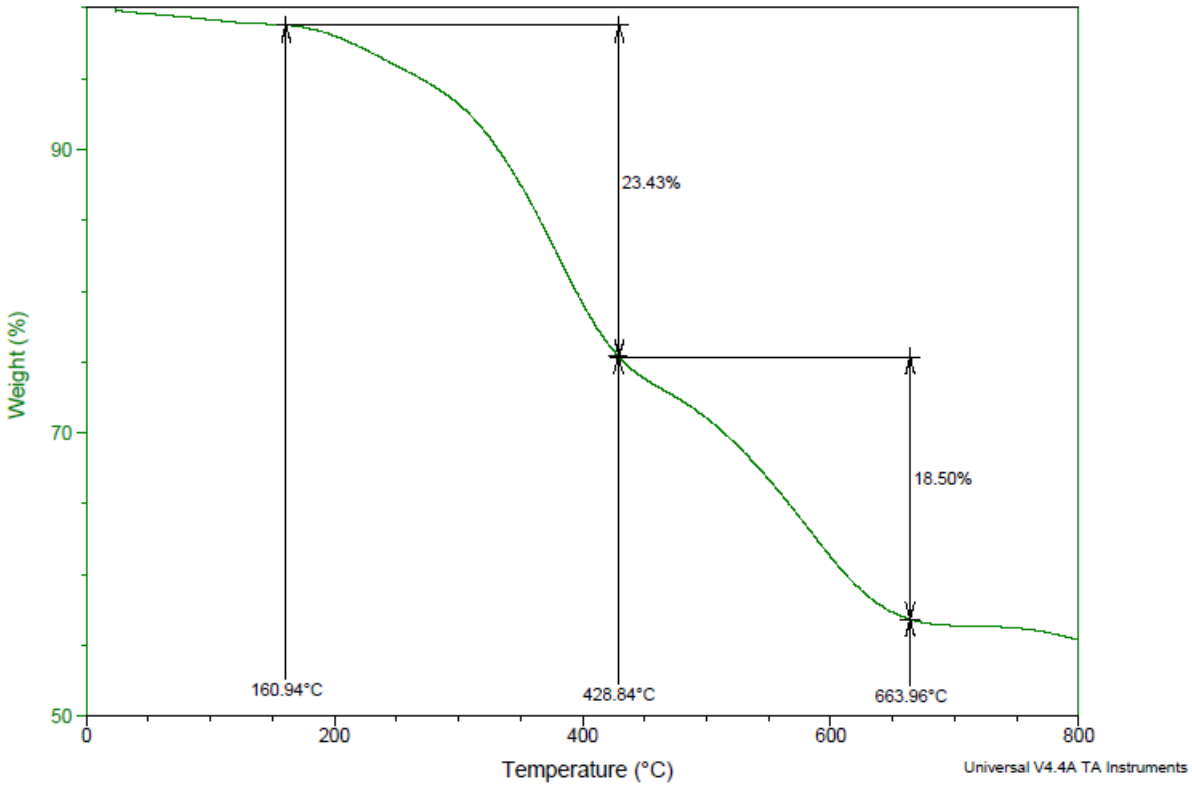

Figure A-3: TGA plot of BC-amine-SSQ particles

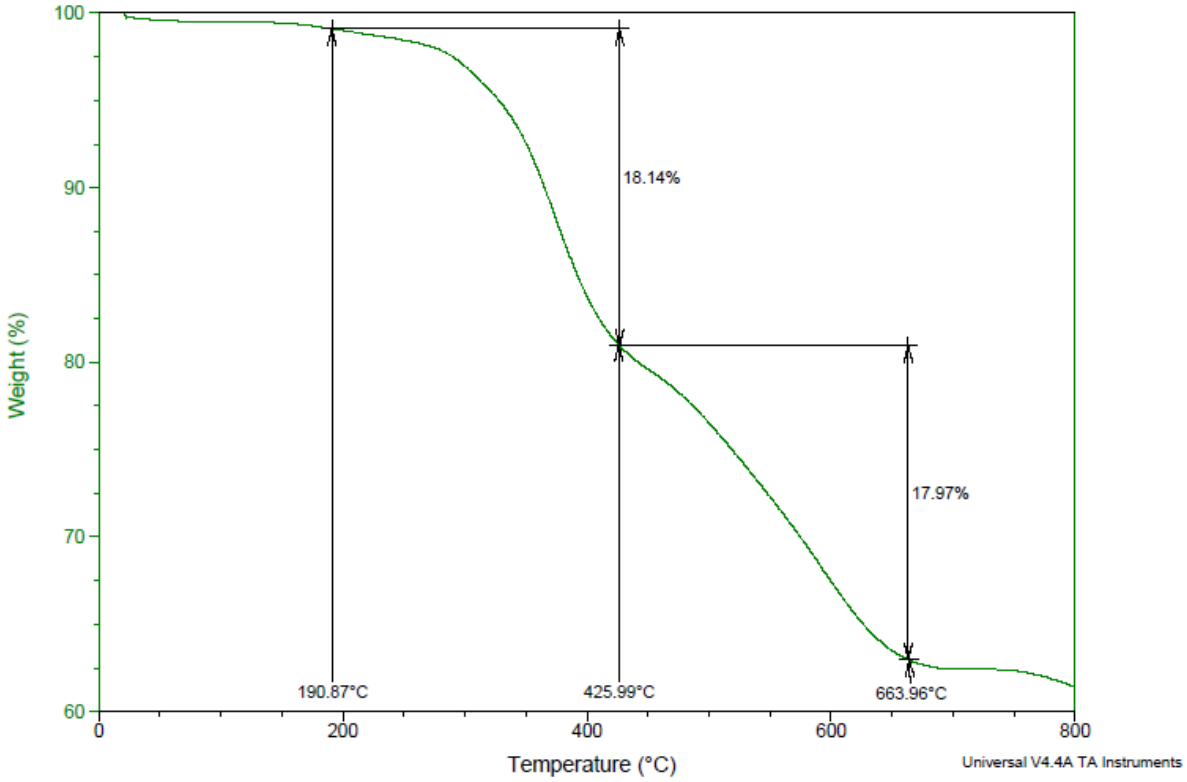

Figure A-4: TGA plot of anthracene and rhodamine functionalized BC-amine-SSQ particles

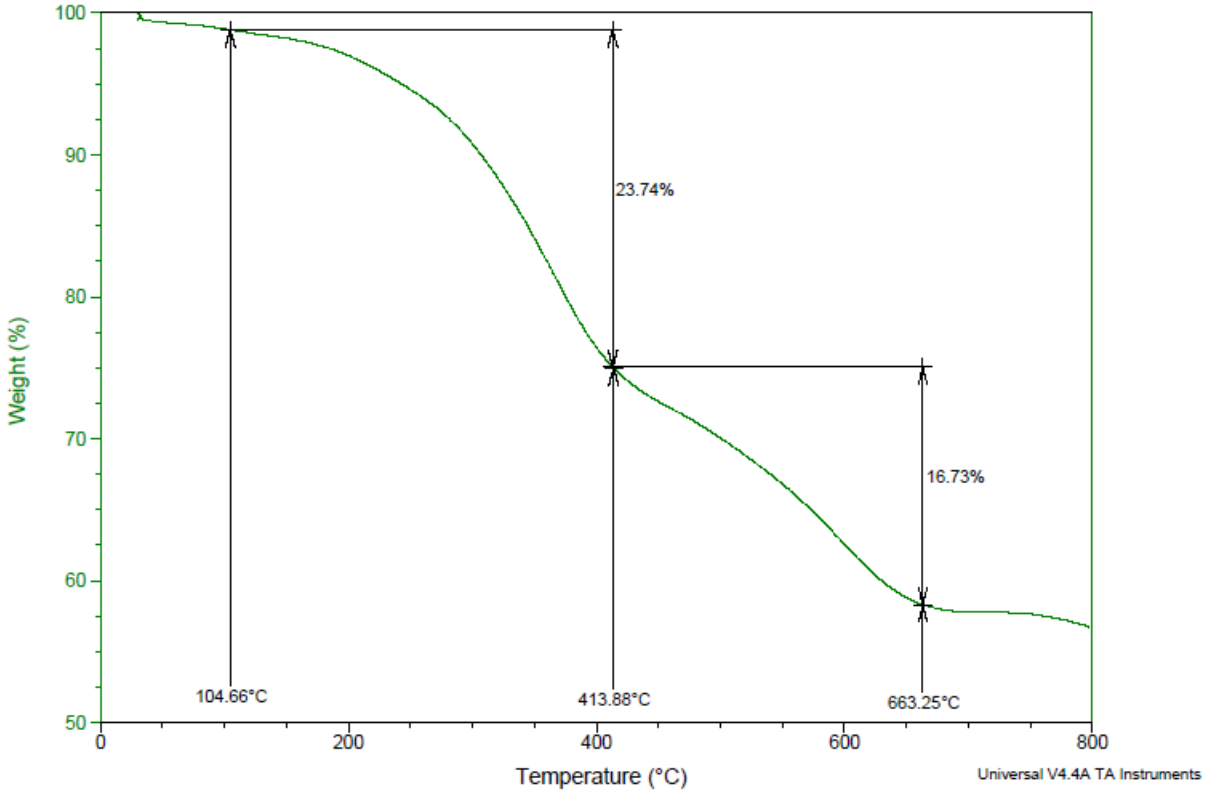

Figure A-5: TGA plot of rhodamine functionalized BC-amine-SSQ particles

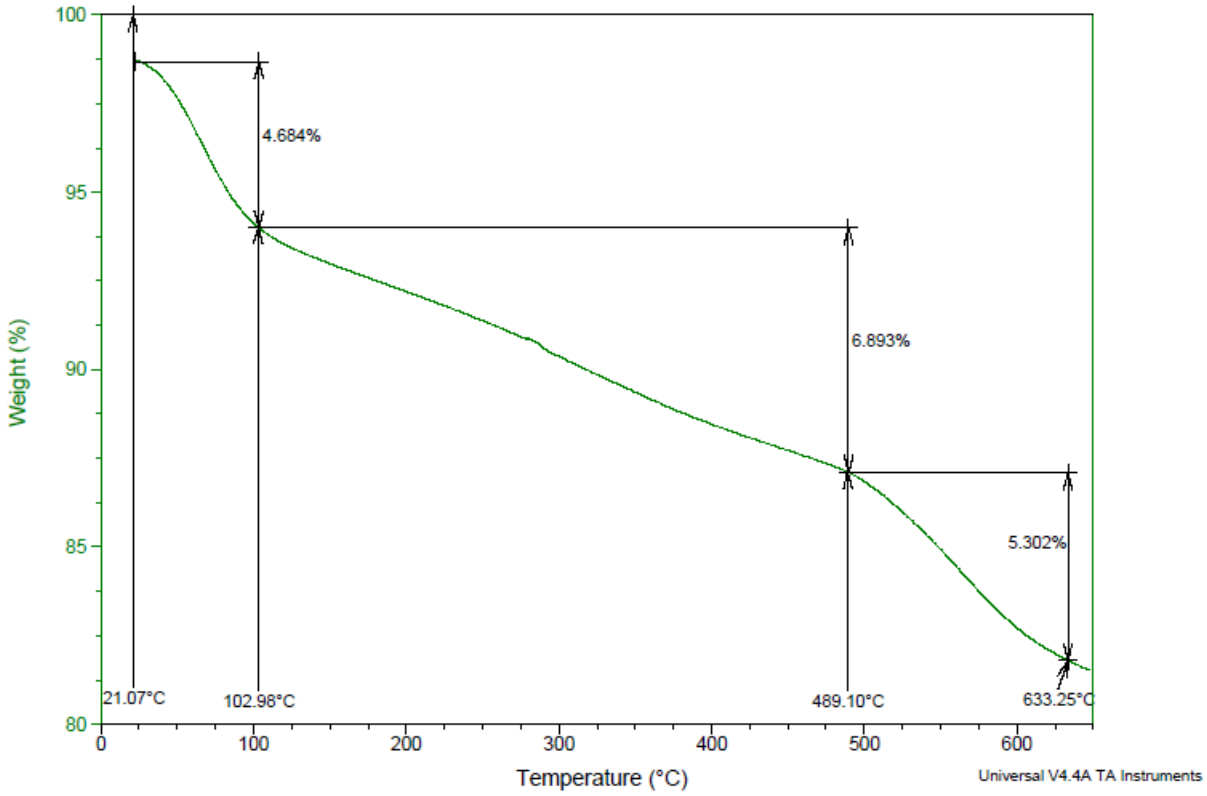

Figure A-6: TGA plot of amine-SSQ particles

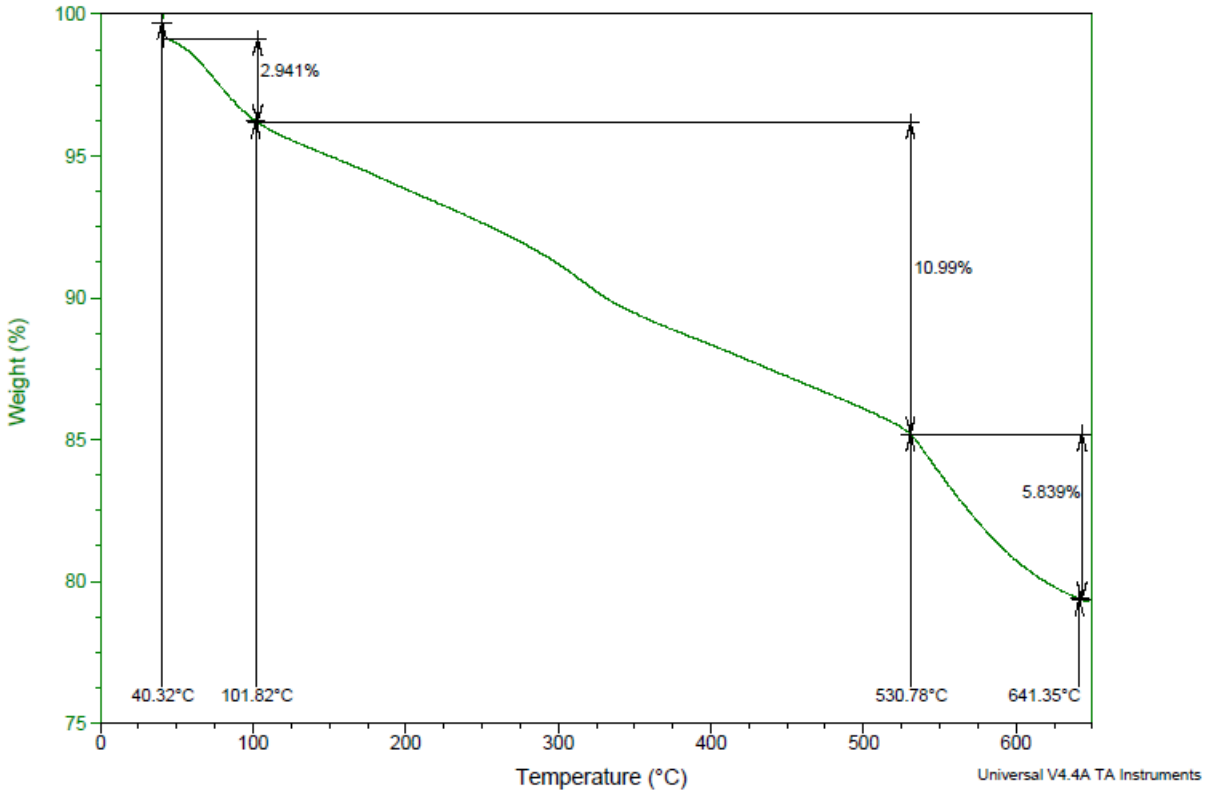

Figure A-7: TGA plot of fluorescein functionalized amine-SSQ particles

REPRODUCIBILITY TABLES

Table A-1: Repeated experimental conditions and morphologies of BC-SSQ particles

Trial # (repeat)	Benzyl chloride trimethoxy silane	Ammonium hydroxide (28%) (mL)	Anhydrous ethanol (200 proof) (mL)	Yield (%)	Size (µm)
1	1.8 mL (8.16 mmol)	1 (7.26 mmol)	10	93.40%	~2-3 µm (round and spherical)
2	1.8 mL (8.16 mmol)	0.5 (3.63 mmol)	10	90.74%	Polymerized
3	1.8 mL (8.16 mmol)	0.25 (1.81 mmol)	10	60.76%	Polymerized
4	1.8 mL (8.16 mmol)	2 (14.52 mmol)	10	83.99%	Polymerized
5	1.8 mL (8.16 mmol)	3 (21.78 mmol)	10	92.88%	Polymerized
6	1.8 mL (8.16 mmol)	4 (29.04 mmol)	10	93.28%	Polymerized
7	1.8 mL (8.16 mmol)	1 (7.26 mmol)	20	94.24%	~0.8 µm and ~2 µm (round and spherical)

8	1.8 mL (8.16 mmol)	1 (7.26 mmol)	30	94.00%	2-3 µm (round and spherical)
9	1.8 mL (8.16 mmol)	1 (7.26 mmol)	40	85.2%	2-3 µm (round and spherical)

Table A-2: Repeated experimental conditions and morphologies of BC-amine-SSQ particles

Trial # (repeat)	**Benzyl chloride trimethoxy silane (mL)**	**3APT silane (mL)**	**Ammonium hydroxide (mL)**	**Anhydrous ethanol (mL)**	**Yield (%)**	**Size (µm)**
1	1 (4.53 mmol)	2 (8.54 mmol)	3.5 (25.41 mmol)	65	20.43%	~1.7-1.9 µm (round and spherical)
2	1 (4.53 mmol)	2 (8.54 mmol)	3.5 (25.41 mmol)	130	15.54%	~1.5-1.7 µm (round and spherical)
3	1 (4.53 mmol)	2 (8.54 mmol)	7 (50.82 mmol)	65	22.53%	~1.2-1.5 µm (round and spherical)
4	1 (4.53 mmol)	2 (8.54 mmol)	1.75 (12.70 mmol)	65	20.49%	~2-2.1µm (round and spherical)

Table A-3: Repeated experimental conditions and morphologies of amine-SSQ particles

Trial # (repeat)	Tetraethoxy silane (mL)	3-APT silane (mL)	Ammonium hydroxide (mL)	Anhydrous ethanol (mL)	Yield (%)	Size (µm)
1	1 (4.47 mmol)	3 (12.82 mmol)	6 (43.56 mmol)	20	20.52%	~0.400 µm
2	1 (4.47 mmol)	3 (12.82 mmol)	8 (58.08 mmol)	20	19.86%	~0.350 µm
3	1 (4.47 mmol)	3 (12.82 mmol)	10 (72.60 mmol)	20	24.73%	~0.350 µm
4	1 (4.47 mmol)	3 (12.82 mmol)	20 (145.20 mmol)	40	15.36%	~0.250-0.3 µm